

Old Dominion University

ODU Digital Commons

Electrical & Computer Engineering Theses &
Dissertations

Electrical & Computer Engineering

Spring 2010

Electric Field Computation of Wet Insulating Surfaces

Bhargavi Sarang
Old Dominion University

Follow this and additional works at: https://digitalcommons.odu.edu/ece_etds



Part of the [Electrical and Electronics Commons](#), [Materials Science and Engineering Commons](#), and the [Power and Energy Commons](#)

Recommended Citation

Sarang, Bhargavi. "Electric Field Computation of Wet Insulating Surfaces" (2010). Master of Science (MS), Thesis, Electrical & Computer Engineering, Old Dominion University, DOI: 10.25777/94pt-2w78 https://digitalcommons.odu.edu/ece_etds/508

This Thesis is brought to you for free and open access by the Electrical & Computer Engineering at ODU Digital Commons. It has been accepted for inclusion in Electrical & Computer Engineering Theses & Dissertations by an authorized administrator of ODU Digital Commons. For more information, please contact digitalcommons@odu.edu.

**ELECTRIC FIELD COMPUTATION OF WET INSULATING
SURFACES**

by

Bhargavi Sarang
B.E. June 2005, University of Wolverhampton

A Thesis Submitted to the Faculty of
Old Dominion University in Partial Fulfillment of the
Requirements for the Degree of

MASTER OF SCIENCE

ELECTRICAL ENGINEERING

OLD DOMINION UNIVERSITY
May 2010

Approved by:

Vishnu K. Lakdawala (Director)

Prathan Basanna (Co-Director)

Linda Vahala (Member)

ABSTRACT

ELECTRIC FIELD COMPUTATION OF WET INSULATING SURFACES

Bhargavi Sarang
Old Dominion University, 2010
Director: Dr. Vishnu K. Lakdawala

High voltage outdoor insulators form the backbone of modern power systems and therefore play a pivotal role in reliable supply of power. The presence of water droplets/films due to rain, fog, etc. enhances the electric field intensity and leads to electrical breakdown subsequently affecting the longevity of the insulator. The magnitude of surface E-fields necessary for initiation of electrical breakdown is a function of water repellent characteristic of an insulator called hydrophobicity. Thus, knowledge of field distribution around water droplets/films at various hydrophobic levels is significant in designing a better insulating material.

The current research analyzed electric field distributions on wet insulating surfaces under three different scenarios. In the first scenario, a single water droplet on a model insulator is considered with a variation of its contact angle and the insulating material. The second set studied the effect on field distribution in presence of multiple droplets by varying the number, relative positioning and contact angle of the water droplets at extreme levels of hydrophobicity. The last case explored the behavior of water droplets and water films on a practical insulator. Simulation results from Coulomb, a Boundary Element Method based 3-D software, indicated that hydrophobicity is crucial in determining formation of water droplets or water films and hence the stress enhancements that ultimately decide initiation and progression of surface flashover.

Copyright © 2010, by Bhargavi Sarang. All Rights Reserved.

Dedicated to my Dad, Mom, Brother, and all my friends

Thank you all for your unconditional love and support.

ACKNOWLEDGMENTS

I express my sincere gratitude to my advisor Dr. Vishnu K Lakdawala for his continuous support, insightful advice, and motivation throughout my work. Without his constant guidance and support, it would not have been possible to complete this thesis. I feel very lucky to be associated with him.

My special thanks go to Dr. Prathap Basappa for his valuable suggestions and help. I thank Dr. Linda Vahala for serving as my committee member and for putting in her valuable time.

I am grateful to my parents for their unconditional love and support throughout my life and for having faith in my abilities. Finally, I would also like to thank my friends Ram, Anusha, Lalitha, Vinay, Kalyan and Rakesh for the constant encouragement and support.

TABLE OF CONTENTS

	Page
LIST OF TABLES.....	viii
LIST OF FIGURES	ix
 Chapter	
1. LITERATURE REVIEW	1
1.1 SIGNIFICANCE OF OUTDOOR INSULATORS	1
1.2 TERMINOLOGY USED IN INSULATORS.....	2
1.3 TYPES OF OUTDOOR INSULATORS.....	4
1.4 REASONS FOR FAILURE OF OUTDOOR INSULATORS	8
1.5 FACTORS LEADING TO THE FLASHOVER OF INSULATING SURFACES.....	17
1.6 NEED FOR ELECTRIC FIELD CALCULATIONS WITH RESPECT TO WATER DROPLETS.....	22
1.6 NUMERICAL TECHNIQUES EMPLOYED IN ELECTRIC FIELD CALCULATIONS.....	23
1.8 OBJECTIVE OF THE THESIS AND DOCUMENTATION OUTLINE.....	25
 2. ELECTRIC FIELD COMPUTATION OF A SINGLE WATER DROPLET ON A MODEL INSULATOR.....	 28
2.1 MOTIVATION.....	28
2.2 MODEL SETUP	29
2.3 CONTACT ANGLE	31
2.4 RESULTS AND ANALYSIS.....	33
2.5 SUMMARY	42
 3. ELECTRIC FIELD COMPUTATION OF MULTIPLE WATER DROPLETS ON A MODEL INSULATOR.....	 43
3.1 MOTIVATION.....	43
3.2 MODEL SETUP	44
3.3 RESULTS AND ANALYSIS.....	46
3.4 SUMMARY	50
 4. ELECTRIC FIELD COMPUTATION WATER DROPLETS ON A PRACTICAL INSULATOR.....	 51
4.1 MOTIVATION.....	51
4.2 MODEL SETUP	51
4.3 RESULTS AND ANALYSIS.....	53
4.4 SUMMARY	62

Chapter	Page
5. CONCLUSIONS AND FUTURE WORK	63
5.1 CONCLUSION OF THE THESIS	63
5.2 FUTURE WORK.....	64
REFERENCES	65
VITA	73

LIST OF TABLES

Table	Page
3.1 E_{\max} for Different Configurations with Respect to Contact Angle of 40°	47
3.2 E_{\max} for Different Configurations with Respect to Contact Angle of 170°	50

LIST OF FIGURES

Figure	Page
1.1 Illustration of Important Dimensions for Insulators.....	3
1.2 Hydrophobicity Demonstrated by Beading..	6
1.3 Flashover Phenomenon on a Polymeric Insulator.....	11
1.4 Experimental Circuit for the Study of Townsend Discharge.....	13
1.5 Cathode Directed Streamer.....	16
2.1 Models Used in Simulation.....	29
2.2 Sheath Configuration Developed using Coulomb.....	30
2.3 Shed Configuration Developed using Coulomb.....	30
2.4 Contact Angle.....	32
2.5 Contact Angle Measurements.....	33
2.6 Equipotential Contour Plot around a Water Droplet with a Contact Angle of 170° for the Sheath Model.....	34
2.7 Equipotential Contour Plot around a Water Droplet with a Contact Angle of 10° for the Sheath Model.....	35
2.8 Variation of Normalized Maximum Electric Field Values with Respect to the Contact Angle for Sheath Region.....	35
2.9 Equipotential Contour Plot around a Water Droplet with a Contact Angle of 170° for the Shed Model	37
2.10 Equipotential Contour Plot around a Water Droplet with a Contact angle of 10° for the Shed Model.....	38
2.11 Variation of Normalized Maximum Electric Field Values with Respect to the Contact Angle for Shed Region.....	39
2.12 Variation of Normalized Maximum Electric Field Values with Respect to the Contact Angle for Sheath configuration.....	40

Figure	Page
2.13 Variation of Normalized Maximum Electric Field Values with Respect to the Contact Angle for Shed Configuration.....	41
3.1 Sheath Configuration.....	44
3.2 Top View Showing the Droplet Arrangement.....	45
3.3 Variation of E_{\max}/E_{avg} with Number of Water Droplets for 40° Contact Angle.....	46
3.4 Variation of E_{\max}/E_{avg} with Number of Water Droplets for 170° Contact angle.....	49
4.1 High Voltage Post Insulator (138 KV).....	52
4.2 Electric Field Distribution along the Insulator Length in the Dry Case.....	53
4.3 Single water droplets placed on a high voltage insulator.....	55
4.4 Electric Field Distribution Due to the Presence of Single Water Droplets on the Shed Region.....	56
4.5 E_{\max} Values for Six Different Cases.....	57
4.6 Water Films Placed on the Shed Regions.....	60
4.7 Electric Field Distribution Due to the Presence of Water Films on the Shed Regions.....	61

CHAPTER 1

LITERATURE REVIEW

This chapter gives an introduction to the basic concepts and terminology that form the foundation of this thesis and also provides a brief review on the work done in the general area of this research.

1.1 Significance of Outdoor Insulators

The supply of inexpensive and reliable electrical energy has become necessary for the economic development of any nation. Power can be transmitted by using either outdoor lines or underground cables. Underground transmission is expensive in nature and thus a network of outdoor lines operating at high voltages is currently the most sought-after method for power delivery [1]. A number of such networks are already functional in industrialized areas and more of such networks are being constructed in developing ones. The distance covered by these networks is in terms of thousands of kilometers. To keep line losses at a minimum, high voltages are used. The distribution networks and secondary networks step the power down and deliver it to the consumers. The high voltage-carrying outdoor line conductors require support structures. At the same time, there is a need for the conductors to be isolated from the support structures that are at ground potential. High voltage insulators are used for both purposes i.e. to support and to isolate the line conductors from the support structures [2,3].

Today's electric power system consists of sophisticated machines that are linked with transmission and distribution systems in a highly complex manner. Due to the integration between the generation, transmission and distribution systems, components

used should be highly reliable so that disturbances in the supply of power to customers are at its minimum. A failure of components in any of the equipment functional zones may lead to power outages. A power outage is generally acceptable if the loss incurred to the customer is negligible. However, power outages, even for a brief period, are undesirable in industrialized areas as they lead to interruption in the production and sometimes to failure of the equipment and thus significant losses are incurred by the customer [4]. According to a survey made by [5], a power interruption of 0.25 seconds to a paper plant in the United States results in a loss of more than \$100,000 excluding legal liabilities. High voltage insulators used in the power stations and on overhead lines play a vital role in causing power outages. Thus, there is a need to develop reliable insulators to provide uninterrupted electricity to the customers.

1.2 Terminology Used in Insulators

A high voltage insulator is described as “a system of components consisting of dielectric or insulating material, terminal electrodes or end fittings and internal parts that help attach the dielectric to the electrodes” in [3]. The terminology used for describing the dimensions of high voltage insulators is fittingly defined in [3,4] as follows:

- (a) *Dry arc or strike distance* is “the shortest distance through the surrounding medium between terminal electrodes, or the sum of the distances between intermediate electrodes, whichever is shorter”.
- (b) *Connection Length* is “the shortest distance between the conductor and the support structure. This includes the strike distance plus the hardware dimensions”.

- (c) *Leakage or Creepage Distance* is “the sum of the shortest distances measured along the insulating surfaces between the conductive parts.”
- (d) *Protected Leakage Distance* is “the distance of the parts of the insulator surface that are not directly exposed to natural elements like sun, wind and rain.”
- (e) *Shaft or Sheath Diameter* is “the measure of the insulator size at its most narrow part.”
- (f) *Shed Diameter* is “the measure of the insulator size at its widest part.”
- (g) *Shed Spacing* is “the distance between the centers of the tips of each shed.”

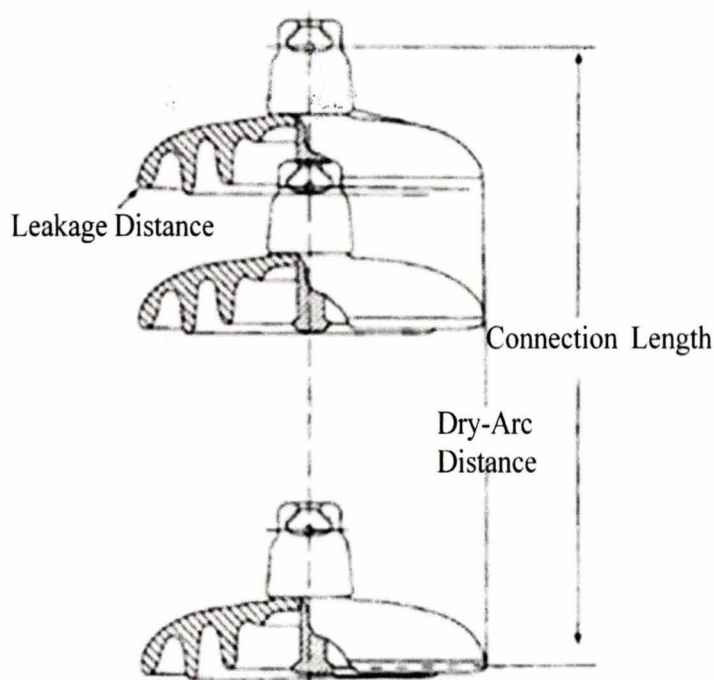


Fig 1.1 Illustration of Important Dimensions for Insulators [3]

1.3 Types of Outdoor Insulators

Outdoor insulators are categorized into two main groups based on the type of dielectric material used to construct them. They are (i) ceramic insulators and (ii) non-ceramic insulators (NCI).

1.3.1 Ceramic Insulators

The need for outdoor insulators originated soon after the invention of telegraph so that grounding out of telegraph lines is avoided. Later, outdoor insulators became a crucial component in the supply of electrical power. Many attempts were initially made with materials such as shellac, cotton soaked with tar, silk, gutta percha, etc. Later it was observed that the glass door knobs performed well and many models were developed with glass [6]. The two main models with glass were the pin type and the cap and pin type models. More information about these models is provided in [3,7]. Glass being brittle in nature is toughened by adding a residual compressive layer on the surface that allows it to tolerate more tension when compared to porcelain. The toughened glass insulator has advantages such as high dielectric strength, lower coefficient of thermal expansion and ease in detection of flaw owing to its transparent body. One main disadvantage of glass insulators is the fact that the moisture condenses on the surface of the insulator very easily resulting in high surface leakage currents and thus is rarely used above 33KV [8,9].

Another dielectric material that came into origin during the same period is porcelain. Glass and porcelain insulators are grouped together as ceramic insulators. Ceramic insulators such as porcelain insulators are known to possess strong electrostatic bonds between atoms so that they exhibit high resistance to heat from electrical

discharge. They are less susceptible to chemical attacks [10]. A negative aspect of this quality is that the strong electrostatic bonds impart a very high value of surface free energy and thus makes the surface of the ceramic insulator easily wettable which is not feasible in contaminated conditions. Another shortcoming of porcelain is that the dense and brittle nature of the material makes the insulators very heavy and prone to breakage [3]. According to [11], 30% of porcelain insulators are estimated to break during transportation and installation excluding the damage during its service.

1.3.2 Non-ceramic Insulators

Today along with the ceramic materials such as glass and porcelain, polymeric or non-ceramic materials are also being used at a large rate. This relatively new technology has already captured almost 20% of the US transmission line market according to [12]. The usage of non-ceramic insulators began in the 1940's and began revolution in outdoor insulating systems [13]. The NCIs reduced the weight of the outdoor insulators drastically. They weighed 90% less than the conventional ceramic insulator and being lighter in weight enabled lighter towers and longer spans of towers [14, 15]. Polymers are less prone to breakage which resulted in a major reduction in the costs for transportation, construction and maintenance. They are smaller in size when compared to ceramic insulators which aids in trimming down the height of the towers [11]. Reduction in vandalism and the ability to resist a mechanical shock are few of the other advantages of NCIs.

Polymeric materials have large molecules that are loosely bonded atoms by Van-der-Waals forces because they exhibit low surface energy [4]. This allows them to possess a peculiar property called *hydrophobicity* that is defined as “ability of the

material to resist the flow of water on its surface” [16]. This property causes water to form beads and run off the surface of the insulator, aiding in cleaning the contaminants on the surface of the insulator without any manual interference. This phenomenon is more preferable than forming a continuous wet sheet, wherein the contaminants combine with the wet sheet and form a conductive layer [17]. With the enormous growth in the pollution levels over the past few years, insulators with hydrophobic properties are suitable over the ceramic insulators. Hydrophobicity is a function of the *contact angle* i.e. the angle between the air, water droplet and the surface of the insulator [16]. A variation of the contact angle implies a change in the hydrophobic level of the insulator which in turn will affect the electrical performance of the polymeric insulator. Figure 1.2 demonstrates the beading of the water droplets on a polymer insulator.



Fig 1.2 Hydrophobicity Demonstrated by Beading [18]

The main disadvantage of polymeric insulators is that they are prone to deterioration by heat, chemicals, electrical discharges, sunlight etc. due to the weak bonds

present between the molecules and may cause *aging*. This is described as “an irreversible and a permanent change” [3]. This implies that composite insulators are more prone to unalterable changes with respect to electrical and mechanical properties.

The three most commonly used polymeric materials for constructing outdoor insulators are silicone rubber, ethylene propylene diene monomer (EPDM) and EPDM/silicone alloy [19]. Among the three, silicone rubber is the most dominant polymeric insulation material and its use in high voltage outdoor insulators is growing at a very fast rate. A brief description about the structure of silicone rubber and its advantages over other polymeric materials is provided below.

Silicone Rubber

Silicone rubber is a synthetic material with a molecular structure based on polydimethylsiloxane (PDMS) and consists of repeated silicon-oxygen atoms with two methyl groups attached to each silicon atom. Hence, it is described as an organo-silicon compound. The silicon-oxygen backbone offers advantages such as the ability to withstand changes in temperature and increased resistance to oxidation and deterioration due to ultra violet rays when compared with the other polymeric materials [20].

Silicone rubber exhibits better hydrophobic levels due to the low surface energy. The material is bestowed with a unique surface property; it has the ability to regain its hydrophobic property after being subjected to contamination or other types of electrical discharges [11]. This type of behavior is believed to exist due to the diffusion of low molecular weight of PDMS according to [21, 22].

1.4 Reasons for Failure of Outdoor Insulators

Outdoor insulators under service conditions experience failure in performance when the surface of the insulator is subjected to mechanical and electrical stresses. These stresses are attributable to either man-made or natural reasons. They are hazardous to the longevity of the insulator as they may cause changes to the physical and chemical properties of an insulator. This subsequently may lead to breakdown of the insulator. Breakdown due to mechanical and electrical stresses are termed as mechanical breakdown and electrical breakdown respectively which are described in detail in the sections below.

1.4.1 Mechanical Breakdown

The ability to withstand the mechanical stresses determines the mechanical strength of the insulator. In the case where the dielectric, end fittings, or the attachments of the dielectric fail to withstand the mechanical stresses, a mechanical breakdown occurs. A consequence of this mechanical failure is dropping of the conductors, which is undesirable as it may lead to power outage for a long period of time and possible injury or damage might also take place.

Factors Influencing Mechanical Breakdown

The factors influencing mechanical breakdown are as follows from references [3, 23, 24].

- Vertical pressure due to the weight of the conductor and horizontal pressure due to the tension of the conductor.
- Ice imposes additional loading. The mechanical load is increased by 20% to 50% by ice alone.
- Wind causes horizontal force on the insulator.

- Cantilever or bending load in supporting the conductor.
- Torsional or twisting type of load during the line construction.
- Vibrational loads due to conductor vibration and movement.
- Shock or impact load due to natural events like earthquakes, ice shedding or man-made events like the impact of vehicles on poles and vandalism (gun shots).
- The mechanical stresses also vary depending on the profile of the insulator and the climatic conditions of the service location.

There is a need to identify the mechanical strength of a dielectric to prevent power outages and the consequent losses. Researchers have already come up with standard tests such as the Combined Thermal and Mechanical Performance tests (T&M), Combined Electrical and Mechanical Failing Load test (M&E), the Rockwell B Hardness (RBH) test etc. to test the reliability of the insulators [25]. The ability of the insulator to endure mechanical stresses is directly proportional to the value of the mechanical strength of the insulator and thus the user can choose an insulator depending on the atmospheric conditions of the service area.

1.4.2 Electrical Breakdown

Outdoor insulators are subjected to high voltages in a continuous manner due to which the reliable electrical performance of insulators becomes a characteristic of pivotal importance. The electrical performance of high voltage outdoor insulators depends on the dielectric strength of the insulating material and the electric stresses developed when exposed to high voltages [3].

Electric Stresses

The electric stress to which an insulating material is subjected to is given by the following equation from [26].

$$E = -\nabla\varphi \quad (1-1)$$

Here in this equation E is the electric field intensity, φ is the applied voltage and ∇ is given by

$$\nabla = a_x \frac{\partial}{\partial x} + a_y \frac{\partial}{\partial y} + a_z \frac{\partial}{\partial z} \quad (1-2)$$

where a_x , a_y and a_z are the components of the position vector.

The electric field distribution is determined by the following equation known as the Poisson's Equation.

$$\nabla^2\varphi = \frac{\rho}{\epsilon_0} \quad (1-3)$$

Here φ is the potential at a given point, ρ is the space charge density in the region, and ϵ_0 is the electric permittivity of the space (vacuum). In the absence of space charges the potential distribution is governed by the Laplace's Equation:

$$\nabla^2\varphi = 0 \quad (1-4)$$

In the above equations the operator ∇^2 is known as the Laplacian and is a scalar with properties:

$$\nabla \cdot \nabla = \nabla^2 = \frac{\partial^2}{\partial x^2} + \frac{\partial^2}{\partial y^2} + \frac{\partial^2}{\partial z^2} \quad (1-5)$$

The phenomenon of electrical breakdown takes place when the electric field intensity exceeds a certain critical value which consequently leads to the failure of the insulator [27].

Dielectric Strength

The dielectric strength of the insulating material is defined as the “maximum dielectric stress the material can withstand” [26]. Surface properties of the insulating material play an important role in preserving the dielectric strength of the insulator [3].

Outdoor insulators used for the purpose of power transmission are surrounded by air and are exposed to the environment because of which surface deposits are formed attributable to pollution, moisture, fog, dew, etc. These deposits act as conducting layers and an increase in the electric field intensity along the surface of the insulator takes place. This leads to ionization of air that is followed by electrical discharges. Furthermore, it affects the dielectric strength of the insulator by decreasing the resistivity values of the dielectric by several orders of magnitude.



Fig 1.3 Flashover Phenomenon on a Polymeric Insulator [29]

An insulator with low dielectric strength becomes more susceptible to failures. Failure caused by surface deposits is termed as *flashover* and is defined as “a disruptive discharge through air around or over the surface of solid insulation, between parts of different potential or polarity, produced by the application of voltage wherein the breakdown path becomes sufficiently ionized to maintain an electric arc” [4]. Figure 1.3 illustrates the flashover phenomenon on a polymeric insulator. The section below explains the physics related to this type of electrical breakdown and the factors leading to this phenomenon.

Physics of Electrical Breakdown

A gas in normal state acts like a perfect insulator. Nevertheless, when a high voltage is applied between the two electrodes in a gaseous medium, the gas becomes a conductor and an electrical breakdown occurs.

Non-sustaining discharges and sustaining discharges are the two types of electrical discharges in gases. When a non-sustaining discharge transforms to a sustaining discharge a breakdown termed as the spark breakdown occurs [26]. Currently, two types of theories namely (i) Townsend Theory and (ii) Streamer Theory are known to explain the mechanism of electrical breakdown [28]. They are described briefly in the sections below.

(i) Townsend Theory

The Townsend Theory states that the initiation of the breakdown process is due to the ionization by collision. Ionization is defined as “the process of liberating an electron from a gas molecule with the simultaneous production of a positive ion” [26]. Ionization process by collision can be explained as follows.

Let us consider a low pressure gas column in which electric field 'E' is applied across two plane parallel plates which is shown in Figure 1.4. Then the electrons that are occasionally formed at the cathode end will drift towards the anode. During this process the electrons gain more energy as they collide with other gas molecules and thereby ionize the gas producing more number of electrons. Multiplication of electrons in this manner creates an electron avalanche that evolves in time and space as it approaches the anode [27, 30]. When $\varepsilon > V_i$, this reaction can be expressed as



Where ε is the energy gained during travel from the cathode to the anode, V_i is the energy required to dislodge an electron from its atomic shell, A is the atom, A^+ is the positive ion and e^- is the electron.

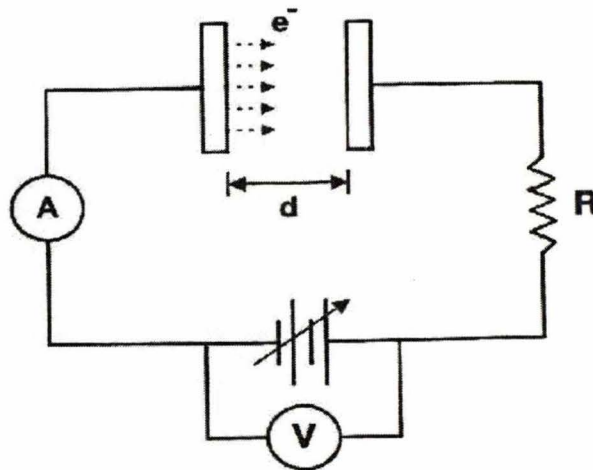


Fig 1.4 Experimental Circuit for the Study of Townsend Discharge [2]

According to Townsend, secondary ionization processes take place which generates secondary electrons and they sustain a discharge giving rise to multiple avalanches. Townsend derived current growth equations for both cases i.e. a single and a

multiple avalanche scenarios which are given below. Townsend's current growth equation for a single avalanche case is:

$$I = I_0 \exp(\alpha d) \quad (1-7)$$

Here α called Townsend's first ionization coefficient depends on gas pressure and represents the average number of ionizing collisions made by an electron per centimeter traveled in the direction of the field, d is the distance or the gap between the cathode and the anode and I_0 is the initial current at the cathode [28].

Townsend's current growth equation for multiple avalanches case is:

$$I = \frac{I_0 \exp(\alpha d)}{1 - \gamma [\exp(\alpha d) - 1]} \quad (1-8)$$

Here γ called Townsend's secondary coefficient which again depends on gas pressure and represents the total number of secondary electrons produced per incident positive ion, photon, excited particle or metastable particle, α is the Townsend's first coefficient and d is the distance between the electrodes.

The equation above gives the total average current in a gap before the occurrence of breakdown. With the increase in the gap, d the denominator of the equation tends to zero. Let us assume that at a distance $d = d_s$ the denominator equals zero and this causes the current I to tend to infinity. This condition is known as the Townsend's Breakdown Criterion which is given below.

$$1 - \gamma [\exp(\alpha d) - 1] = 0 \quad (1-9)$$

Or is given by

$$\gamma [\exp(\alpha d) - 1] = 1 \quad (1-10)$$

Since the value of $\exp(\alpha d)$ is usually very large, the equation is simplified as

$$\gamma [\exp(\alpha d)] = 1 \quad (1-11)$$

The value of the voltage at which the Townsends first and second coefficients α and γ satisfy the breakdown criterion is called the spark breakdown voltage V_s and the corresponding distance d_s is termed as the sparking distance.

Practical experiments showed that Townsend Theory had drawbacks such as

- Assumption that current growth occurs only due to ionization process whereas essentially it was found to depend on the gas pressure and the distance between the electrodes.
- Prediction of time lags to be of the order of 10^{-5} s when in fact breakdown occurs at very short time lags which are of the order of 10^{-8} .
- Discharges were in practice found to be filamentary and irregular in contrast to the prediction made by Townsend as the discharge being in a diffused form.

(ii) Streamer Theory

Townsend Theory's drawbacks led to the development of another theory namely the Streamer Theory which could successfully explain the above mentioned phenomena by Raether. Around the same time Meek and Loeb also proposed a similar theory.

Raether and Meek and Loeb, predicted that the space charge developed by a single avalanche leads to the transformation of the avalanche into a plasma streamer. This can be explained as follows according to [26, 2, 28, 30].

Let us consider a single electron starting from the cathode moving towards the anode which builds up an avalanche due to ionization collision. It is known that the process of ionization generates a positive ion along with the electron and that the rate at

which the electron traverses towards the anode is much more when compared with the positive ion. Thus the electrons will get absorbed by the anode at a very fast rate and the positive ions which are left behind form a positive space charge at the anode. This process leads to the intensification of space charge field. Once it reaches the magnitude of the initially applied field, it produces more electrons consequently giving rise to secondary avalanches. This further enhances the charge density and third generation of avalanches is formed and so on. These avalanches are continuously absorbed by the primary avalanche and the positive space charges traverse towards the cathode at a very fast rate forming an ionized channel from anode to cathode. This ionized channel is called the streamer. This process is depicted in the Figure 1.5. When the streamer tip touches cathode, a stream of electrons is produced to neutralize the positive charge. This results in the formation of a spark and thus the spark breakdown occurs.

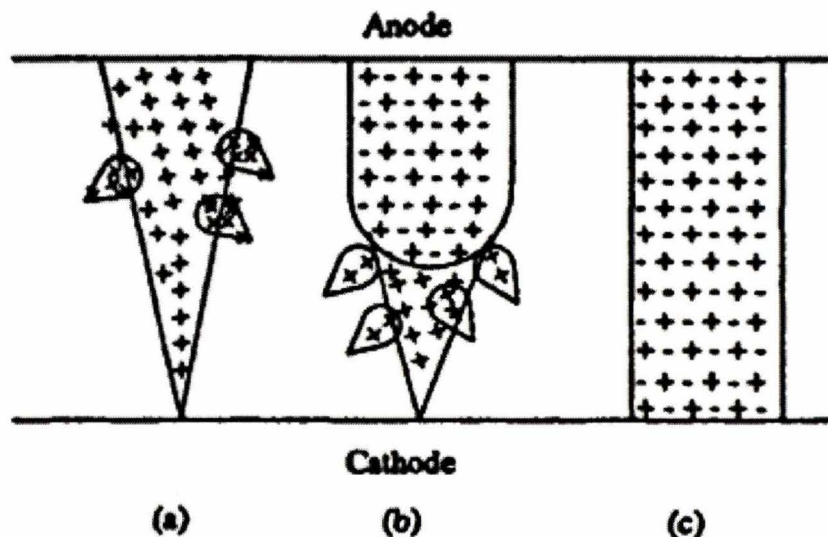


Fig 1.5 Cathode Directed Streamer [26]

According to Raether [30], when the transition from an avalanche to a streamer takes place at a gap distance or the distance between the cathode and electrode of d cm, the breakdown criterion is

$$\alpha d = 17.7 + \ln(d) \quad (1-12)$$

He proposed that at a critical avalanche length, x_c , where the value of $\exp(\alpha x_c)$ is high enough for the avalanche to get developed into a streamer, if $x_c < d$, streamer mechanism is observed and if $x_c > d$, Townsend's mechanism is observed.

Meek obtained the breakdown criterion to estimate the electric field at which an avalanche gets transformed into a streamer as follows:

$$E = 5.28 \times 10^{-7} \frac{\alpha \exp(\alpha d)}{\left(\frac{d}{p}\right)^{\frac{1}{2}}} \quad (1-13)$$

Or in logarithmic form it can be written as

$$\frac{\alpha}{p} pd + \ln\left(\frac{\alpha}{p}\right) = 14.46 + \ln\left(\frac{E}{p}\right) - \frac{1}{2} \ln(pd) + \ln(d) \quad (1-14)$$

Here E is the electric field, d is the length of the gap, p is the gas pressure in Torr, and α is the Townsend's first ionization coefficient [28].

1.5 Factors Leading to the Flashover of the Insulating Surfaces

The factors leading to flashover are mainly (i) pollution and (ii) water droplets/films which are briefly described below.

1.5.1 Pollution

Contamination on the surface of insulators on account of pollution introduces leakage currents and an increase in its intensity can lead to eventual flashover of the insulator. Based on the service experience, flashover caused from pollution is considered

to be a major problem for outdoor insulators used in high voltage transmission [31]. Contaminated surfaces do not conduct under dry conditions and thus contamination is of little concern during dry periods [29]. However the moist surfaces under fog or rain conditions dissolve the contaminants and form conductive layers on the surface of the insulator.

The nature of the contaminants varies depending on the environmental conditions of the area in service. Examples of typical pollution environments and the contaminants are listed below [4]

- A marine environment where in contaminants such as Na, Cl, Mg, K and other marine salts get accumulated owing to the presence of sea.
- An industrial environment introduces soluble pollutants such as dust, soot etc from quarries, cement factories, electric generating stations burning coal or oil, refineries etc.
- An agricultural environment causes pollution in the form of soluble fertilizers along with relatively insoluble dust and chaff.
- A desert environment suffers with pollutants such as sand and high degree of salt in some areas.

The two main factors that decide the performance of outdoor insulators in polluted environments are: (a) The type of the insulating material and (b) The profile of the insulator

(a) Type of the Insulating Material

A ceramic insulator owing to its hydrophilic property forms water films on the surface of the insulators or in other words wets the surface completely and the deposited

salts gets dissolved in the water. This gives rise to continuous conducting electrolyte films that enhances the leakage currents and consequently leads the insulator to complete flashover [32]. In highly polluted areas, ceramic insulators mainly suffer from pin erosion and result in dropping of lines.

A non-ceramic insulator exhibits better performance in contaminated areas when compared with a ceramic insulator as it is endowed with the property of hydrophobicity which enables self-cleaning of the insulator. The discharges occur only at very high levels of contamination [33]. Nevertheless, polymeric insulators suffer from problems such as erosion, tracking, etc. due to the weakly bonded atoms and loss of hydrophobicity due to ageing [3].

(b) Profile of the Insulator

The profile of the insulator is a crucial factor in determining the pollution performance of the outdoor insulator. The main factors involved in designing an insulator that would contribute to better contamination performance are listed below according to [1, 3, 34, 35, 36, and 37].

- Tests on contaminated insulators have suggested that an increase in the leakage distance of the insulator enhances the AC and DC withstand voltages and thereby improves the efficiency of the insulators in contaminated regions. Usage of leakage extenders is recommended by [3] to increase the leakage distance of the insulators.
- Researchers have proposed different profiles depending on the environment and the nature of the contaminants. With respect to the shed profile, open profile or aerodynamic designs have been found to work well in desert type environments

whereas insulators with more corrugated ribs improve pollution performance in fog type environments. It has been observed that an insulator with a combination of large-size and small-size skirts withstands more alternating voltage in areas with high precipitation.

- Protected leakage path should be considered when designing the sheds of the insulator which plays a major role in improving the functioning of the insulators in terms of tracking and erosion.
- The author in [1] believes that a significant improvement can be achieved by modifying the shapes of the insulators in the direction of lesser interference with incident air flow.
- The profile of the insulator should enable self-cleaning of the contaminants.
- In addition to the above mentioned factors the shed spacing to the shed diameter ratio, the shed inclination angle are other profile parameters that should be considered for superior contamination performance.

Standardized tests such as the salt-fog test and clean-fog test have been developed to learn about the contamination performance of various insulators. The contamination severity is expressed in terms of Equivalent Salt Deposition Density (ESDD) which will enable comparison of the effectiveness of insulators with respect to contamination [3].

1.5.2 Water Droplets/Films

Pollution plays a significant role in causing flashover of an insulator. However it has been noticed that presence of water droplets and films lead to the flashover of an insulator even under the absence of actual contaminants.

The behavior of the hydrophilic-based ceramic insulators in the presence of water films has already been mentioned in the sections above. Non-ceramic insulators, silicone rubber in particular, exhibits excellent hydrophobic property which enables self-cleaning of the contaminants. Nevertheless the presence of water droplets over a silicone rubber insulator surface creates locations of high electric field intensity, a region where the electrical breakdown can initiate [38]. The influence of water droplets on the flashover mechanism along a hydrophobic insulator surface is explained below.

Water droplets may be present over the outdoor insulators either due to fog, dew or rain and their presence drops the dielectric intensity and increases the field intensification [39]. The electric field in the tangential direction causes the water droplets to get deformed and elongate along the direction of the electric field. This creates a force on the surface of the droplet and subsequently gives rise to micro discharges which is followed by electro-chemical deterioration of the insulator surface. Solvable nitrates resulting in a higher conductivity of the water droplets will appear. When E-field value exceeds the breakdown strength of air, *partial discharges* occur which are defined as “an electric discharge that does not completely bridge the space between two conducting electrodes”. Occurrence of partial discharge in air is generally termed as *corona*. The partial discharges propagate across dried regions or bands leading to dry bands being formed on the insulator surface. The dry bands demonstrate greater resistance compared to the wet surface and the voltage stress is concentrated across the dry bands. Thus, a significant change in the voltage distribution takes place along the insulator. As the surface is wetted further, the electric stress across the dry bands increases and causes the discharge current to increase to a point where the discharges elongate and join together to

bridge the gap between the insulator terminals. A power arc is formed and eventually leads to the flashover of the insulator [3,34]. Corona and arcing can cause serious damage to the insulator surface and therefore accelerates the ageing process of an insulator. This may lead to a loss in the level of hydrophobicity, which is the most important feature of the insulator.

Depending on the amount of loss in the level of hydrophobicity, a corresponding change in the contact angle of the water droplet takes place. When the insulator completely loses the property of hydrophobicity the water droplet is deformed from bead-like to a film. Attributing to the weak bonds, the surface of the polymeric insulators is more affected by the electrical discharges when compared with the ceramic insulators and may result in relatively poor performance. This situation enhances the aging process of the polymeric insulator and thus measures are to be taken to avoid the loss of hydrophobicity.

1.6 Need for Electric Field Calculations with Respect to Water Droplets

Currently in the USA, non-ceramic insulators especially silicone rubber insulators which are endowed with superior hydrophobic qualities are being used extensively for termination of distribution cables in the power supply. Although it is a known fact that polymeric insulators display excellent short-term mechanical and dielectric properties they are still affected by long-term degradations originated due to the action of electric stresses. A prediction of flashover of polymeric insulators is of major concern since they have less on-field experience when compared with the ceramic insulators and thus there is a need for more research in this area. At present, there are no standardized tests

available to calculate the flashover voltage of polymeric insulators due to water droplets or films under the absence of contaminants. Moreover laboratory experiments are often time consuming and expensive. Based on the facts above, it becomes necessary to study and understand the electric field distribution around water droplets/ films on silicone rubber insulators so that one can predict the electrical breakdown strength of an insulator and subsequently take measures to avoid breakdown [29]. Electric field calculations can be made by using either analytical or numerical methods. However analytical methods work well only in the case of simple systems. Numerical methods on the other hand provide an optimal and an accurate solution to both simple and natively complex systems. Therefore the use of numerical methods is recommended to calculate electrical field values around water droplets/films on an insulator surface.

1.7 Numerical Techniques Employed in E-field Calculations

An electric field analysis can be conducted using either analytical or numerical techniques. Analytical techniques generate accurate solutions for calculating electric fields in simple insulating systems. Nevertheless, in the case of realistic insulating systems which are natively complex, numerical techniques serves as the only alternative approach for field analysis.

Many numerical methods such as the Charge Simulation Method (CSM), the Finite Difference Method (FDM), the Finite Element Method (FEM), the Boundary Integration Method, and the Boundary Element Method (BEM) have been developed to calculate electric field intensities [40].

CSM is a method in which the simulation of an actual electric field is conducted with a field formed by a finite number of imaginary charges situated inside conductors or outside the desired field region. This method works well in systems without singular points but its application is limited because of the difficulties that arise in solving the fields consisting of very thin conductors [41].

FDM is a method that allows replacement of the differential equations describing electric potential by finite difference equations and solves it by an iterative process. The limitations of this method include crude modeling of geometry, excessive computational time and a large number of unknowns [42].

Unlike FDM, in the Finite Element Method, the governing equations are integrated over each finite element and the solution is summed over the entire problem domain. A few of the shortcomings of FEM are that it is not well suited for open region problems, truncation of space, high probability of introducing discontinuities in the derivative of potentials in the geometric model and problems caused due to extreme aspect ratios [43].

The drawbacks mentioned in the above methods led to the development of Boundary Element Method. Moreover these methods can be applied only in bounded regions whereas many of the physical problems of interest are unbounded. This method involves the “transformation of the partial differential equations describing the behavior of the variables, inside and on the boundary of the domain under consideration, into integral equations relating only boundary values” [44]. These integral equations are based on Green’s Formula and the result is considered to be an exact solution of the

governing partial differential equation. The main advantages of this method according to references [44, 45] are listed below.

- In comparison with other numerical methods, for BEM the numerical discretizations are restricted only to the boundaries which results in a reduced number of linear system of equations and thereby makes data generation relatively easier.
- Green's Formula enables the method to work accurately for problems with unbounded domains without causing truncations. An accurate calculation of the field at any point in space can be done.
- BEM, owing to the use of 2-dimensional elements on the surfaces, allows the user to set up a problem in a quick and an easy manner. Only the elements on interfaces or assigned boundary conditions are involved therefore problem modifications become hassle free.
- Since BEM is based on Green's Theorem, error analysis can be achieved by checking if the solution satisfies the boundary conditions on all boundaries or not.

Based on the advantages mentioned above BEM is considered to be an efficient method in performing electric field calculations on high voltage insulating surfaces.

1.8 Objective of the Thesis and Documentation Outline

From the previous sections of this Chapter it can be stated that water droplets/films lead to the breakdown of the insulator even under the absence of actual contaminants. The overall objective of this thesis is to study the effect of water droplets and water films on the surface of the overhead insulators (porcelain and silicone rubber).

Their contributions to modifications to the electric field distribution and hence possibility of failure is investigated while considering the following different scenarios:

- A single water droplet on the surface of the insulator with a variation of insulating materials and contact angles.
- The affect of multiple water droplets with respect to the change in number and relative position on the sheath part of the insulator at extreme hydrophobic levels.
- The behavior of water droplets and water films on a practical insulator. Here formation of the water films indicates complete deterioration of the hydrophobic property.

The thesis is organized as follows:

Chapter 2 describes the shed and the sheath model insulators considered to accomplish the present work. Both, the contact angle and the insulating material are varied. Subsequently, the results and discussions are provided in this chapter.

Chapter 3 illustrates seven different arrangements with single and multiple water droplets on the surface of the sheath model insulator. Three parameters namely contact angle, number and relative positioning of the water droplets are varied and the resultant models are simulated. Two contact angles that exhibit extreme levels of hydrophobicity are chosen. The results and discussions related to the variation of each parameter are provided in this chapter.

Chapter 4 discusses the axi-symmetrical model of the practical insulator used in performing two sets of simulations. The first set constituted variation of water droplets on both the sheath and the shed regions. The second set of simulations looked into the affect

of water films on the shed region of the insulator. This is followed by the results and analysis.

Chapter 5 gives a complete summary of the research work conducted and the conclusions made from the simulations performed. It also discusses work to be done in the future to further advance the research on this topic.

CHAPTER 2

ELECTRIC FIELD COMPUTATION OF A SINGLE WATER DROPLET ON A MODEL INSULATOR

2.1 Motivation

The electric field intensity is at its maximum level at the triple point between water, air and insulator. When a locally high electric field around a water droplet approaches the critical ionization field in air, a corona discharge occurs. Hydrophobicity plays an important role in electric field intensification. It can be described as the property of any material to resist the flow of water on its surface. The contact angle between the water and the insulating surface determines the hydrophobicity of the surface.

To study the effect of water droplets/water films in outdoor insulation, in particular, the effect of hydrophobicity, physical experiments were conducted at the Arizona State University (ASU), Arizona, U.S.A., under the guidance of Dr. Ravi S. Gorur. The experimental results required a benchmark check. Furthermore, investigating the effect of water droplets becomes difficult with physical experiments since the shape of the water droplets keep varying with the E-field. These necessities led to numerical computation of E-field values with the aid of solvers. The credibility of the experimental results obtained at ASU was checked with the simulations performed by the research lab facility at the Old Dominion University (ODU). The electric field distributions are examined using the recent version (Version 6.4) of a 3D-Field BEM based solver Coulomb. However, there is a high probability for the simulated results to be erroneous. To check the validity of the results, a previously researched sheath and shed configuration in [46] with a single water droplet of contact angle 90^0 is cross checked prior to

performing simulations on models with different contact angles.

In this work simulations are performed on a single water droplet by varying the contact angles from 10° to 170° to inquire the effect of contact angle. Another important factor investigated is the difference in electric field intensification between materials having intrinsic hydrophobic properties and the materials that lack hydrophobic properties. The materials used are Silicon Rubber (SIR) and porcelain respectively.

2.2 Model Setup

Water droplets are present on both the shed and sheath parts of a practical insulator. Detecting the changes in the values of the E-field becomes difficult on a practical insulator. Hence, two models that represent the shed and the sheath portions of an insulator namely the Shed and the Sheath models are considered. They are shown in the Figure 2.1 below. The models designed in Coulomb are displayed in the Figures 2.2 and 2.3 respectively.

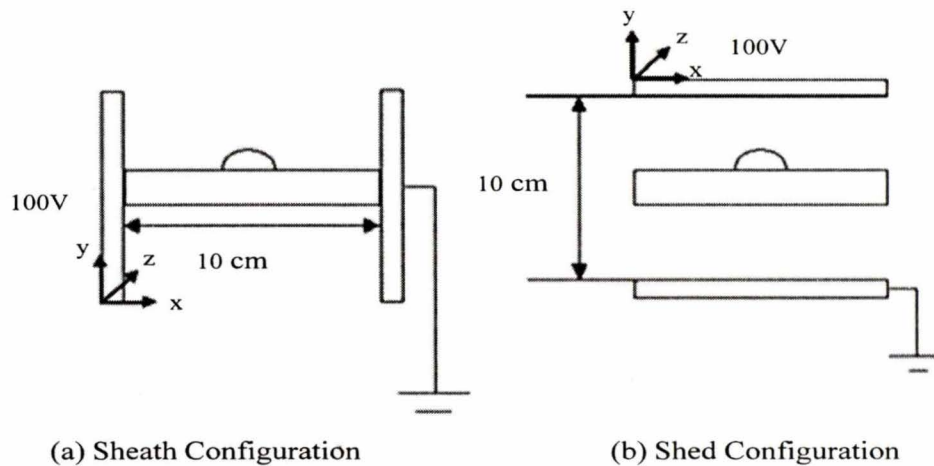


Fig 2.1 Models used in Simulation. ((a) Sheath Configuration (b) Shed Configuration)

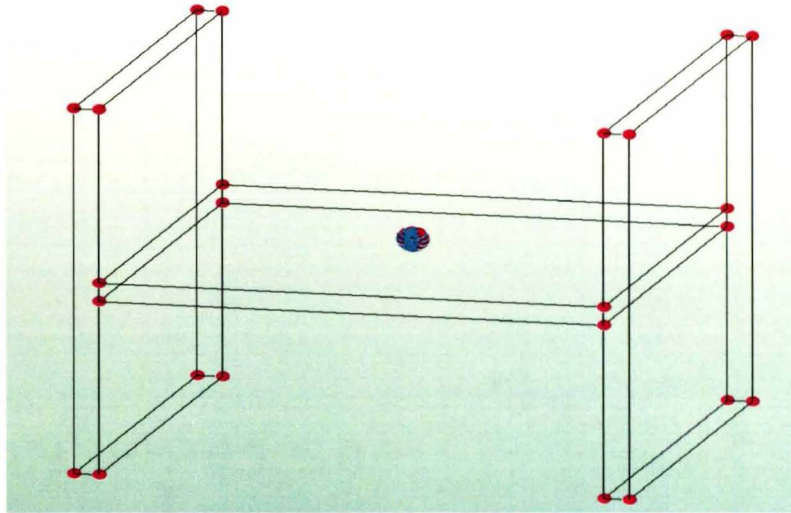


Fig 2.2 Sheath Configuration Developed using Coulomb

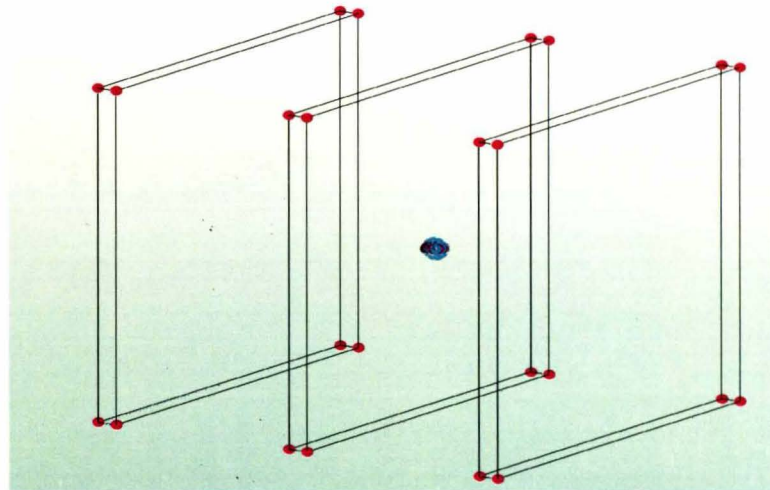


Fig 2.3 Shed Configuration Developed using Coulomb

The Figure 2.1(a) is a sheath configuration with a single water droplet on the surface of the insulator with two electrodes connected perpendicular to the insulator. The dimensions of the insulator are 10-cm x 10-cm with a thickness of 0.5-cm. The dimensions of the electrodes are the same as that of the insulator. The radius of the water

droplet is taken as 2mm. The height of the water droplet is not a constant value as it varies with the contact angle. The values of the dielectric constant and conductivity of the water droplet are considered to be 80 and $2.0e^{-4}$ mho/meter respectively.

The Figure 2.1(b) is a shed configuration with a single water droplet on the center of the insulator surface with two electrodes parallel to the insulator. The dimensions of the insulator, electrodes and the water droplet are similar to that of the sheath configuration. As mentioned earlier the simulations are performed on both the SIR insulator and the porcelain insulator with $\epsilon_r = 6$, $\gamma = 1.0e^{-10}$ mho/meter and $\epsilon_r = 4.3$ and $\gamma = 1.0e^{-4}$ mho/meter respectively.

2.3 Contact Angle

Hydrophobicity is an important property which aids in increasing the longevity of an insulator by allowing the water to form like a bead instead of a sheet or a film on the insulator's surface. Bead-like water droplets prevent the formation of solid conducting areas which turn into flashover prone regions and also help in removing loose contamination from the insulator surface which in turn reduces the leakage currents.

Two methods can be used to measure the level of hydrophobicity of an insulator namely the STRI (Swedish Transmission Research Institute) Method and the Contact Angle Method [17]. In the STRI Method, the hydrophobicity is measured by spraying water on the surface of the insulator and by visually comparing the formation of the water droplets to the seven standard images provided by the STRI guide i.e. HC-1 (completely hydrophobic) to HC-7 (completely hydrophilic) [47]. However the contact

angle measurement method is more widely accepted due to its ability to measure accurately in small increments [17].

The contact angle is the angle ' θ ' between the air, water droplet and the surface of the insulator which is shown in the Figure 2.4 below. On an ideal hydrophobic insulator surface the water droplet takes the shape of a sphere making a contact angle of 180° with the insulating surface and an angle of 0° with an ideal hydrophilic surface. To be more precise all insulators with contact angles greater than 90° are called hydrophobic and contact angles less than 90° are called hydrophilic. This is depicted in the Figure 2.5 below. The aging of the insulator due to corona, arcing etc. causes a loss of hydrophobicity of the insulating material. A reduction in the level of hydrophobicity causes an increase in the electric field intensification. The droplets then would tend to elongate in the direction of the axial field and thereby gets deformed into an ellipsoidal shape. This causes a change in the contact angle. Thus by varying the contact angles of the water droplet with respect to the insulating surface one can observe the variation of E-field at different degrees of hydrophobicity. This will help researchers understand the ageing process of an insulator in a lucid manner.

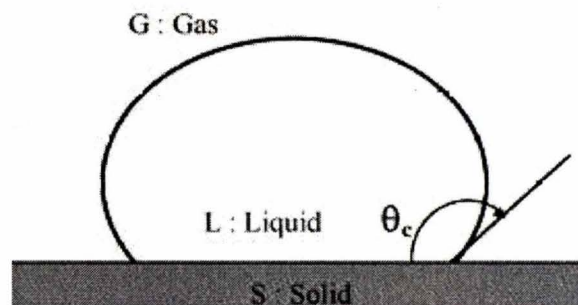


Fig 2.4 Contact Angle [48]

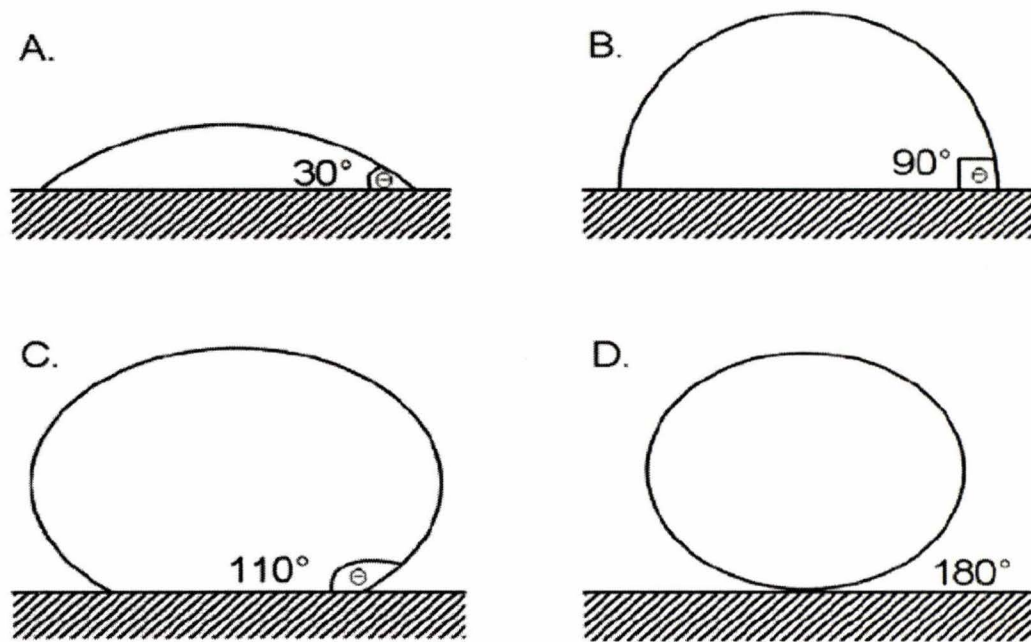


Fig 2.5 Contact Angle Measurements (Hydrophilic Surface - (A), Minimum Hydrophobic Surface - (B), Typical Hydrophobicity for Silicone Rubber - (C) and Ideal Superhydrophobic Surface - (D)) [17].

2.4 Results and Analysis

The results and the analysis are explained in detail in the sections below.

2.4.1 Effect of Contact Angle in the Sheath Region

The sheath region of an insulator attributing to the narrow diameter (width is 5 to 7 times smaller than the shed region) experiences more electrical stress when compared to the shed region. The water droplets across the sheath region near the HV end act as probable locations for initiation of ionization due to the high stress concentration. The direction of the applied voltage is tangential to the sheath region and therefore tangential stresses play a pivotal role in the performance of the insulator. Depending on the level of hydrophobicity the shape of the water droplet varies and consequently affects the

wettability of the insulator surface. Electric field distribution varies with respect to the shape of the water droplet. Therefore to investigate this aspect simulations were conducted on a single water droplet with a variation in the contact angle. A single water droplet is placed on the SIR insulator surface of the Sheath Configuration Model and its contact angle is varied from 10° to 170° to analyze the variation in E_{\max} (maximum value of E-field) around the water droplet.

The Figures 2.6 and 2.7 display the equipotential contour plots of the contact angles 170° and 10° . They indicate the significance of hydrophobicity on an E-field concentration. A contour plot can be described as a graphical picture on which the characteristics of a surface are shown by contour lines. A contour line is a line or a curve which joins points of equal value. A comparison between Figures 2.6 and 2.7 also shows the difference in the shape of the water droplet at different contact angles. At 170° of contact angle, the water droplet is of the shape of almost a sphere and at a contact angle of 10° it forms a film-like structure.

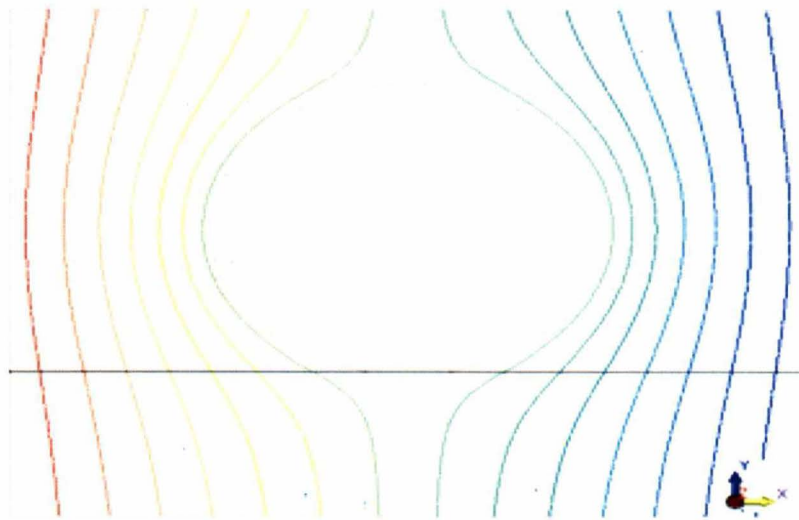


Fig 2.6 Equipotential Contour Plot around a Water Droplet with a Contact Angle of 170°
for the Sheath Model

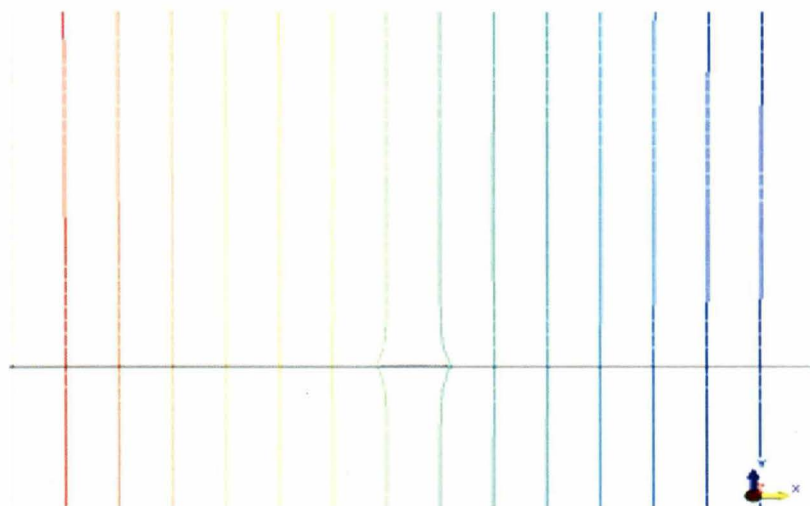


Fig 2.7 Equipotential Contour Plot around a Water Droplet with a Contact Angle of 10°
for the Sheath model

A correlation between the magnitude of the ratio of E_{\max}/E_0 and the contact angles ranging from 10° to 170° on the sheath configuration of a SIR insulator is illustrated in the figure 2.8 below. The maximum E-field value with respect to the contact angle is represented by E_{\max} and the average stress is denoted by E_0 .

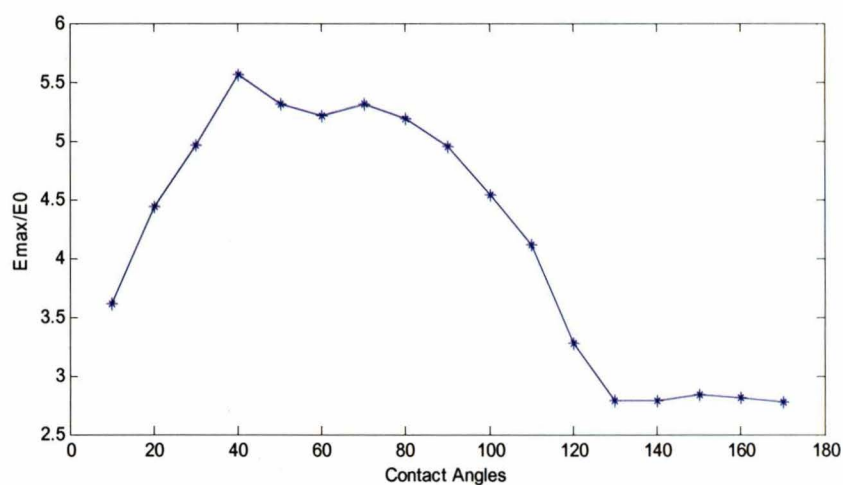


Fig 2.8 Variation of Normalized Maximum Electric Field Values with Respect to the
Contact Angle for Sheath Region

The Figure 2.8 shows that E_{\max} is a function of contact angle. The E_{\max} values are observed to be low initially between contact angles of 10° to 30° . The values of E_{\max} are considerably high between the contact angles ranging from 30° to 90° . E_{\max} reaches its peak at 40° of contact angle indicating that this condition is more prone to flashover when compared to the other cases. The contact angles between 90° and 120° showed a drastic reduction in the amount of stress values and are nearly flattened out above 120° of contact angle.

The explanation for the above mentioned pattern of stress values is given as follows. For water droplets of the same volume, the length of contact with the insulator is longer for those drops of small contact angles and shorter for those of large contact angles [49]. Thus when an insulator surface has a high degree of hydrophobicity the length of the water droplet attached to the surface of the insulator is minimal. At this juncture, the triple point between water drop, insulator and air is engulfed by the water which is an equipotential surface [50] and thus the level of E_{\max} is relatively low. This is experienced by the insulators making contact angles greater than 90° with the insulator surface which is depicted in Figure 2.8.

Due to natural weathering the hydrophobic property of the insulator gradually leaches out and the wettability of the insulator increases. This process signifies a reduction in the contact angle and thus the length of contact is at its maximum. In practice when the contact angle is low it forms a water film on the sheath surface and causes the leakage surface to become wet. This effectively reduces the dry region of the insulator length and causes an increase in the electric field intensification. This explains the high stress values in the range of 30° to 90° of contact angle. Therefore it can be

concluded that the magnitude of the E-field necessary to result in the onset of water drop corona is a function of both drop size and surface hydrophobicity [51].

The E_{\max} values are low for contact angles below 30° due to the resistive grading effect produced by the thin water film [38]. Hence it is most desirable to have a contact angle above 90° , below which the insulator is more vulnerable to wet flashover.

2.4.2 Effect of Contact Angle in the Shed Region

The shed region protects the sheath surface by dispersing water away like an umbrella [8]. The stresses on the shed region in practice are several orders of magnitude lesser than in the sheath region due to the large diameter. Therefore the obtained values do not provide a comparison between the stress magnitudes of the shed and the sheath. Nevertheless, these values enable us to examine E_{\max} variations with respect to different contact angles. The breakdown process can be originated on the shed region under the absence of water droplets on the sheath region. Rain, fog, dew, snow etc causes the water droplets to get accumulated on the shed region.

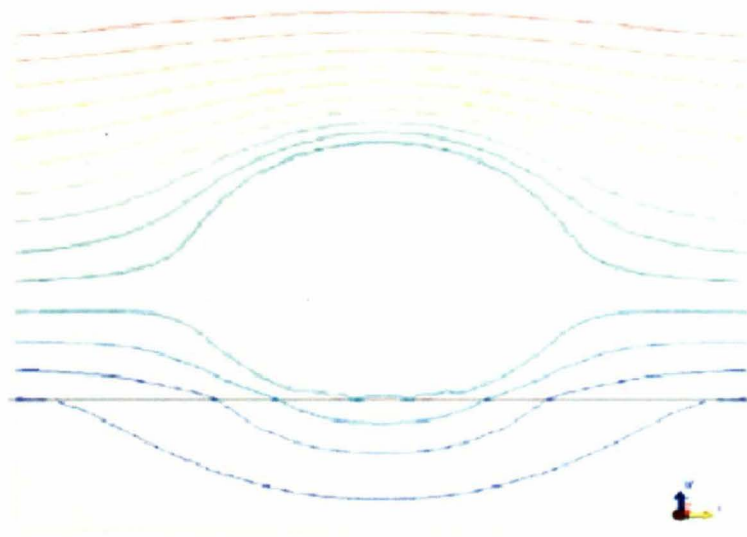


Fig 2.9 Equipotential Contour Plot around a Water Droplet with a Contact Angle of 170°
for the Shed Model

The Figures 2.9 and 2.10 represent the equipotential patterns with contact angles 170° and 10° respectively. It can be observed that the maximum stress occurs at the triple point for a contact angle of 10° and for a contact angle of 170° the maximum stress occurs at around the topmost tip.

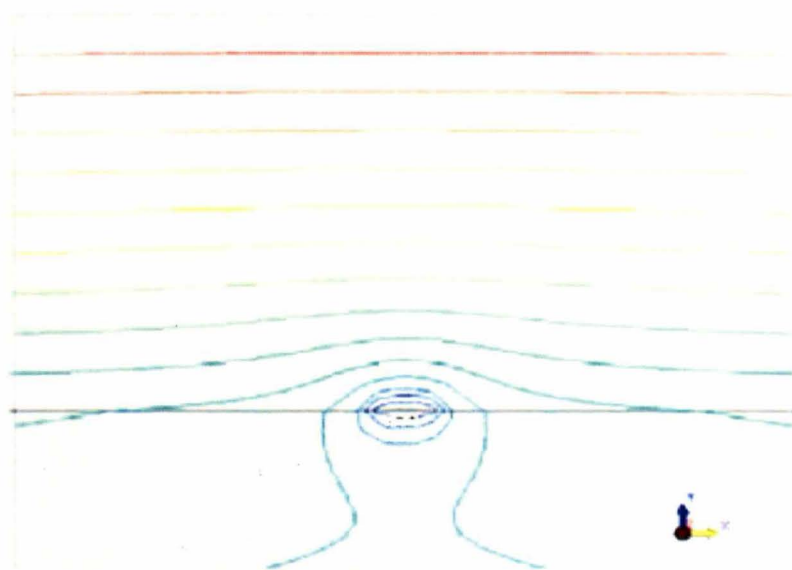


Fig 2.10 Equipotential Contour Plot around a Water Droplet with a Contact Angle of 10° for the Shed Model

The Figure 2.11 provides a graphical representation of variation of the ratio of E_{\max}/E_0 with respect to the contact angles ranging from 10° to 170° on the shed configuration of a SIR insulator. A drastic reduction in the values of E_{\max} is noticed between the contact angles 10° and 40° and above the contact angle of 50° variations are at its minimum. This indicates that at extremely low levels of hydrophobicity, high electric field intensities occur at the triple point and may initiate the ionization process. However, at higher levels of hydrophobicity, it is observed that the maximum electric field occurs at the tip of the bubble which is represented by the contact angles ranging from 50° to 170° here. This behavior is due to the proportional increase in the curvature

of the water bubble with an increase in the angle of contact. Since the maximum stress occurs at the tip of the bubble away from the insulating surface the stress values are relatively small.

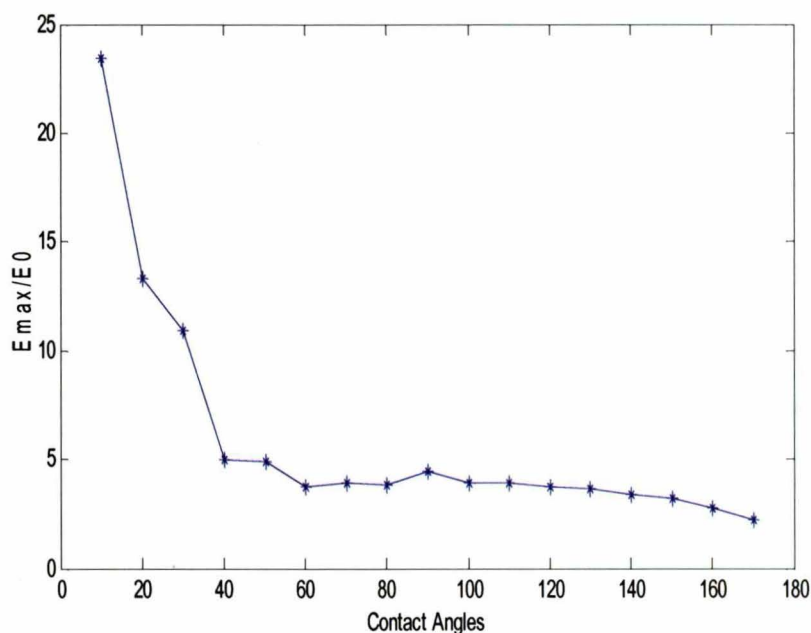


Fig 2.11 Variation of Normalized Maximum Electric Field Values with Respect to the Contact Angle for Shed Region

2.4.3 Effect of Insulating Material

The criterion for design in high voltage insulators depends on the dielectric strength of the insulating materials and the electric field stresses developed in them when subjected to high voltages. These electrical characteristics influence the material aging of the insulator which is very important in high voltage insulators. As mentioned in the previous Chapter, two types of insulating materials namely ceramic and non-ceramic insulators are currently being used. Polymeric insulators exhibit more advantages when compared with ceramic insulators. However, ambiguity lies in terms of relative

performance between ceramic and polymeric insulators. The potential of a NCI in delivering high performance is not known to its fullest extent. To aid in choosing a better operating insulating material simulations are conducted on both ceramic and non-ceramic insulators. The materials used are porcelain and SIR respectively. The E-Field intensification caused by both of these materials on the sheath and the shed regions is compared in the section below.

The figures 2.12 and 2.13 below represent the variation of the normalized maximum electric field values with respect to the contact angles in the range 10^0 to 170^0 for the sheath and the shed configurations respectively. Square points are for porcelain whereas the asterisks represent SIR.

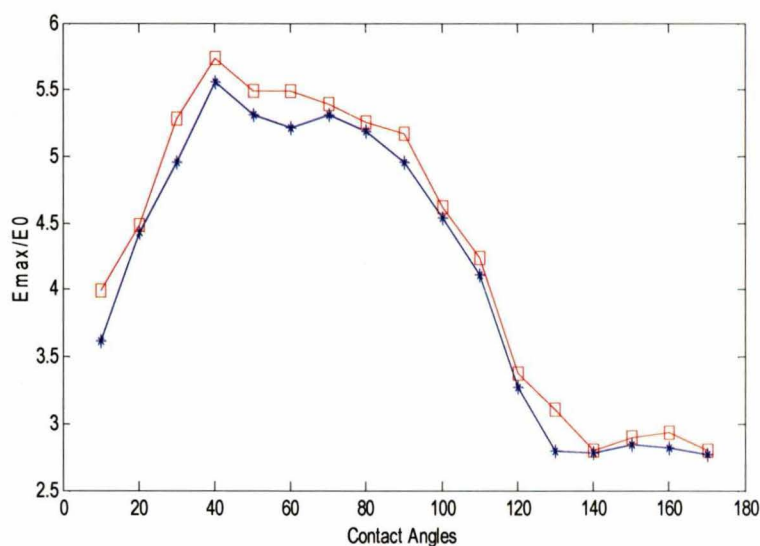


Fig 2.12 Variation of Normalized Maximum Electric Field Values with Respect to the Contact Angle for Sheath Configuration. (Square points are for porcelain and asterisk points are for silicone rubber)

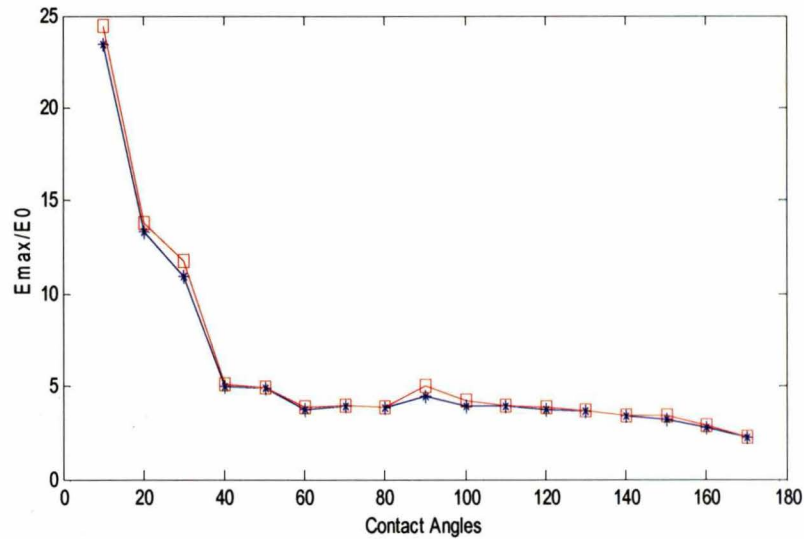


Fig 2.13 Variation of Normalized Maximum Electric Field Values with Respect to the Contact Angle for Shed Configuration. (Square points are for porcelain and asterisk points are for silicone rubber)

The Figures 2.12 and 2.13 shows that the stress values in porcelain are higher than those in SIR. The reasons are given as follows.

- The relative dielectric constant of porcelain is larger than that of SIR.
- Porcelain exhibits low levels of hydrophobicity as compared to SIR.
- Evaporation of water takes more time in porcelain due to the high surface energy and thus results in high stress values.

Higher stress values indicate higher susceptibility to flashover and thus aids in damaging the insulator surface at a faster rate. The above facts and results demonstrate that SIR performs better when compared to porcelain.

2.5 Summary

The influence of hydrophobicity, which is a function of contact angle, and the nature of the dielectric material in increasing the electric stress values are investigated in this Chapter. The simulations performed on a single water droplet on the shed and the sheath configurations with a variation in the contact angle and insulating material indicated the following.

- The stress values around the water droplet on the sheath region are significantly high when compared with the shed region.
- E_{\max} is a function of contact angle.
- The maximum stress value always occurs at the triple point (interface between air, water and the insulating surface) of the water droplet on the sheath region.
- For water droplets on the shed configuration, at low levels of hydrophobicity the maximum stress occurs at the triple point and for high levels of hydrophobicity the maximum stress value shifts to the tip of the water droplet.
- SIR has better electrical performance characteristics when compared with porcelain.

CHAPTER 3

ELECTRIC FIELD COMPUTATION OF MULTIPLE WATER DROPLETS ON A MODEL INSULATOR

3.1 Motivation

In the practical scenario, under service conditions, water droplets get accumulated on the surface of the insulator due to rain, dew, fog etc. With high electric field intensity at the triple point, a water droplet gets elongated in the direction of the electric field. This poses a serious problem in the case of multiple water droplets on an insulator as these elongations shorten the insulating distance considerably. This in turn intensifies the electric field intensity leading to the formation of corona that affects the longevity of the insulator. The number of water droplets and their relative positions also affect the insulating distance. Thus the principle for regulating the electric field in insulator design emanates from studying the increase of electric field with respect to the change in the number and relative placement of water droplets. The previous chapter included the simulations performed around a single water droplet on the surface of the insulator. It was observed that the maximum electric field occurs in the sheath region of the insulator and that the contact angle plays an important role in increasing the electric field intensity. Furthermore, the angles 170° and 40° exhibited the minimum and the maximum amount of E-field respectively. Therefore, the current work placed emphasis only on two sets of simulations at contact angles 40° and 170° that are conducted on the sheath configuration model by varying the number and position of water droplets. The contact angle 40° represents a degraded insulator and 170° serves as an insulator with high degree of hydrophobicity.

3.2 Model Setup

The sheath region being narrower in dimension experiences higher amount of stress when compared to the shed region as seen in the previous chapter. Electric field distribution along the sheath surface is more crucial in determining the breakdown strength of the insulating material when compared with the shed region and therefore the simulations are performed only on the sheath model which is shown below in Figure 3.1. The dimensions of the insulator and the two electrodes are 10 cm x 10 cm with the thickness being 0.5 cm. The radius of the water droplet is taken to be 2 mm and its height varies with the contact angle. The relative dielectric constant ϵ_r of water is taken as 80 and its conductivity $= 2.0e^{-4}$ Siemens. The material used is SIR and its relative dielectric constant ϵ_r , of SIR insulator is taken as 4.3 and its conductivity $\gamma = 1.0e^{-4}$ Siemens.

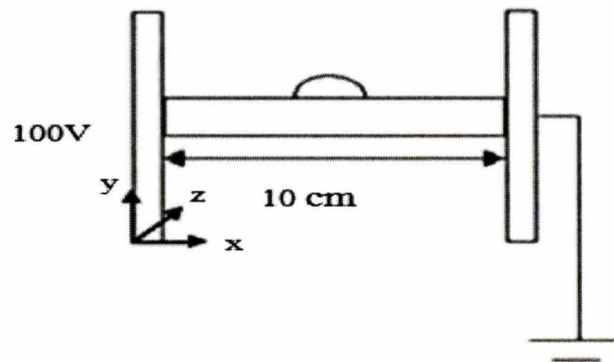


Fig 3.1 Sheath Configuration

Seven different patterns are considered to perform the simulations where the number of droplets, distance between the water droplets and their relative positions are varied which are shown in the Figure 3.2 below. All the models are built using the 3D integrated software Coulomb and the Boundary Element Method is used to solve them.

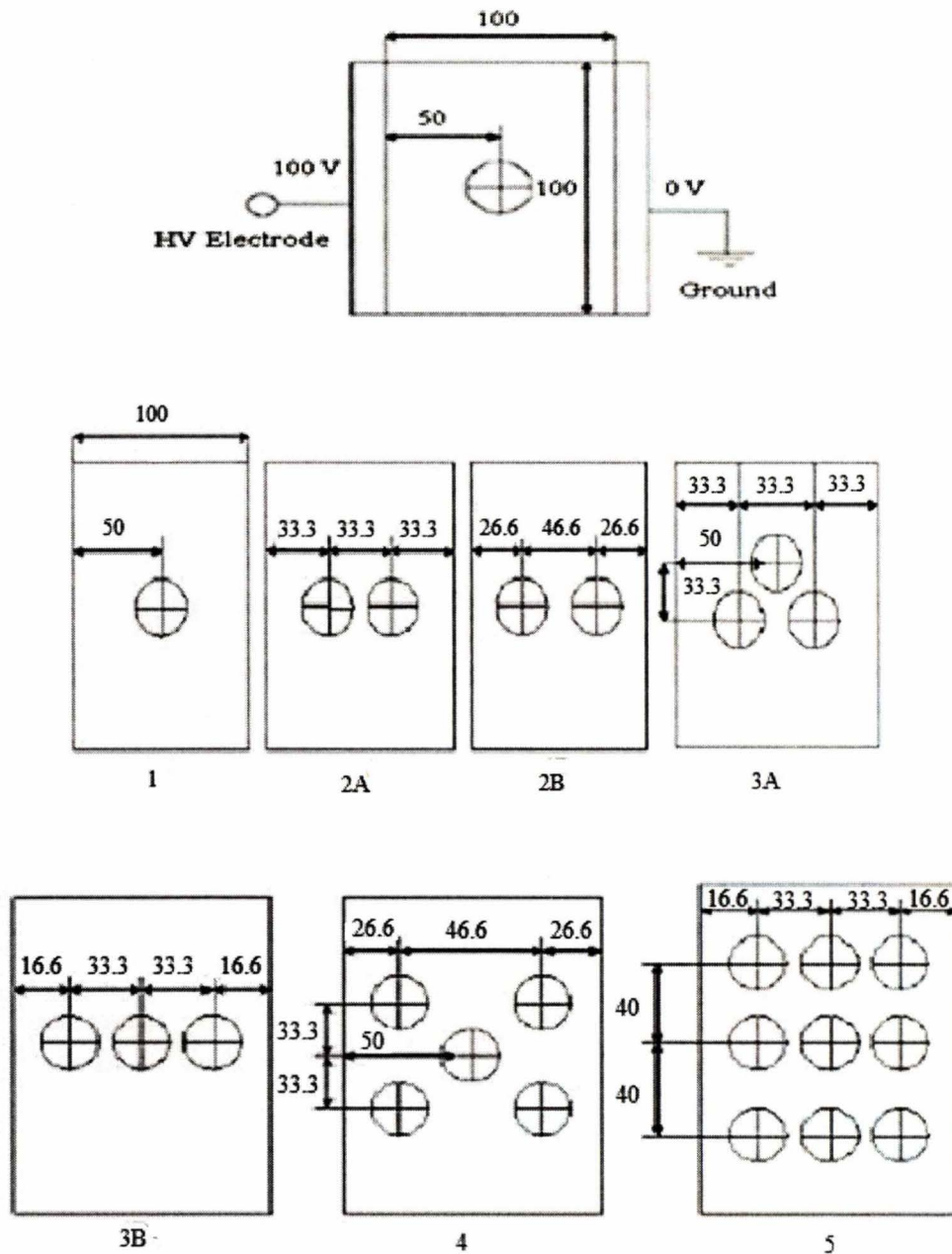


Fig 3.2. Top View Showing the Droplet Arrangement. ((1) single droplet, (2A) two water droplets, (2B) two droplets with larger spacing between them, (3A) arrangement of 3 droplets in the form of a triangle, (3B) 3 droplets in a row, (4) 5 droplets and (5) 9 droplets. All dimensions given are in mm and symbolize the distances of the droplets from the respective electrodes and the distances between them)

3.3 Results and Analysis

The simulation results and analysis are presented in the sections below.

3.3.1 Effect of Multiple Water Droplets on the E-field

The increase in the electric field intensity in context of multiple water droplets is much more important than with a single water droplet. The Figure 3.3 below shows the effect of multiple water droplets placed at different locations on E-field with respect to the contact angle of 40° .

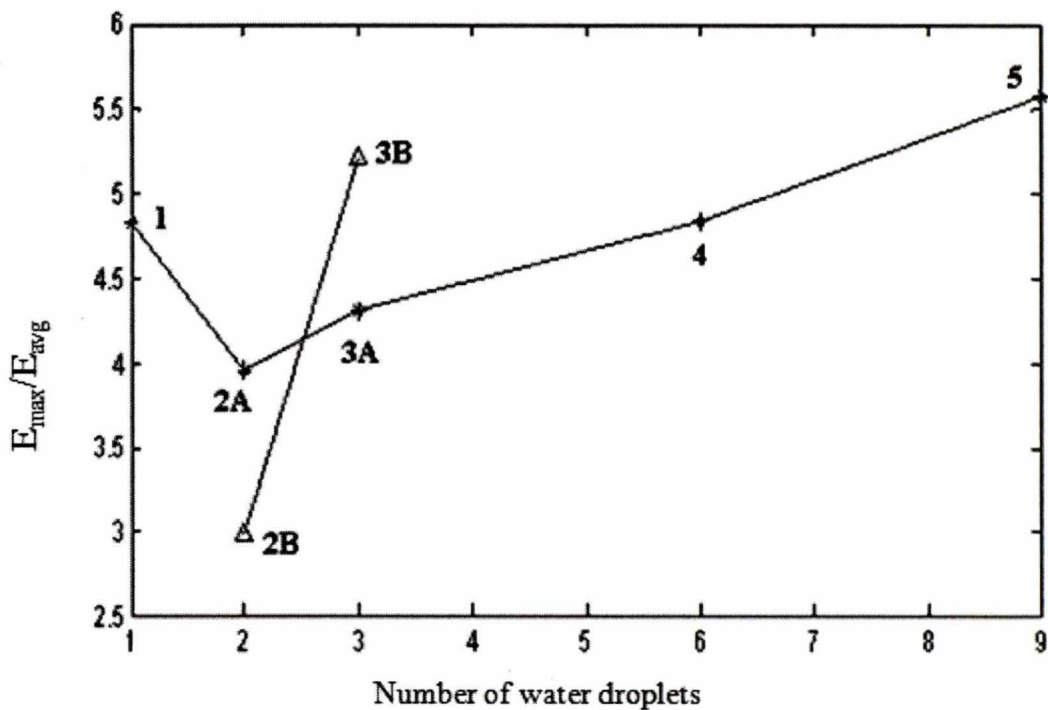


Figure 3.3 Variation of E_{\max}/E_{avg} with Number of Water Droplets for 40° Contact Angle.

(The triangular symbol indicates the results of models 2B and 3B)

The table 3.1 displays the values of E_{\max} for the seven different configurations at contact angle 40° .

Table 3.1 E_{\max} for Different Configurations with Respect to Contact Angle of 40°

Model	1	2A	2B	3A	3B	4	5
E_{\max}	4.824	3.948	2.974	4.305	5.208	4.842	5.578

The effect of distance between two droplets on E_{\max} is analyzed with the help of models 2A and 2B with the distances between their centers 33.33 mm and 46.66 mm respectively. It is seen from Table 1 that the E-field value is lower in the case of 2B when compared to 2A. This is because the droplets behave like equipotential surfaces and when the distance between two droplets is less, the effect on the values of electric field is more and vice versa. Therefore it can be concluded that the value of E_{\max} is inversely proportional to the distance between the water droplets [38].

The effect of relative positioning of water droplets is investigated in Models 3A and 3B. Three water droplets are positioned in the form of a triangle in Model 3A and three water droplets are arranged in a row in 3B with a distance of 33.33 mm between their centers in both of the models. Another factor that has been varied is the distance between the electrode and water droplet. The distance between the first water droplet and the electrode is 16.66 mm and is the same with the last water droplet in 3B. In 3A the distances between the electrode and the water droplet are 33.33mm and 50mm. It can be seen from Table 1 that there is a drastic increase in E_{\max} when the droplets are placed with their centers oriented along the field in contrast to placing them in a triangular fashion. This is because the water droplets attain the potentials of the equipotentials passing through them and act as conducting particles aligned along the field direction resulting in enhanced electric stresses locally. The presence of the water particles effectively reduces the dry region and the voltage between the water particles is

distributed between the dry regions between them. Another reason for the significant increase in the E-field is due to the decrease in the distance between the electrodes and the water droplets [52]. The E-field value depends on the distance between the water droplet and the electrode i.e. the shorter the distance between the droplet and the nearest electrode the higher the E-field intensification [48]. The numerical results indicate that the components of the E-field along the field direction are significantly larger than the other two directions.

From Table 3.1 above it can be observed that $E_{\max}(1) > E_{\max}(3A)$. This is due to the fact that single water droplet causes more non-uniformity than multiple droplets. $E_{\max}(3A) > E_{\max}(2A)$ since the presence of third water droplet affects the stresses at the triple points of both water particles.

The effect of more number of water droplets on E-field is investigated through Models 4 and 5. From Table 3.1 it can be inferred that the position of the droplets and the distances between them along the field of direction is crucial in determining the magnitude and location of E_{\max} . Even though there are five water droplets in Model 4 compared to three in the Model 3B the E-field intensity is not as high as in the case of 3B. This is because the relative distance between water particles is relatively higher in 4 than in 3B.

It can be seen that the E-field is higher in the case of model 5 than the model 4. From Table 3.1 above it can be observed that the $E_{\max}(5) > E_{\max}(3B)$. The increase in the E-field value in Model 5 is attributed to the presence of more water droplets when compared to the Model 3 due to which there is a reduction in the effective flashover distance between both electrodes [52]. The presence of additional water droplets makes

stress distribution more uniform although the electric field strength in the vicinity of each water droplet is enhanced.

The numerical values of electrical stresses depend on the method of computation, degree of discretization, convergence criteria, etc. These values are to be used qualitatively to compare the relative effect due to differences in configurations.

3.3.2 Effect of Contact Angle on the E-field

Simulations for all configurations shown in Figure 3.2 are carried out for the contact angle 170° . The Figure 3.4 below indicates the effect of multiple water droplets placed at different locations on E_{\max}/E_{avg} with respect to the contact angle of 170° . The triangle shape indicates the E-field for Models 2B and 3B.

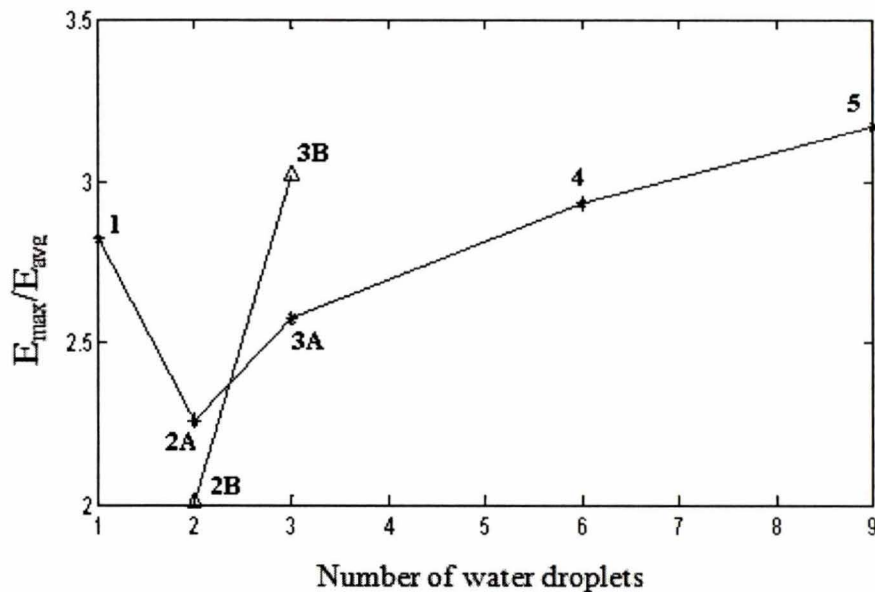


Fig 3.4 Variation of E_{\max}/E_{avg} with Number of Water Droplets for 170° Contact Angle.

(The triangular symbol indicates the results of Models 2B and 3B)

The Table 3.2 displays the values of E_{\max} for the seven different configurations at contact angle 170° .

Table 3.2 E_{\max} for Different Configurations with Respect to Contact Angle of 170°

Model	1	2A	2B	3A	3B	4	5
E_{\max}	2.82	2.259	2.009	2.576	3.021	2.933	3.169

Comparison of Figures 3.3 and 3.4 and tables 3.1 and 3.2 show that except for single water droplet case the ratio of E_{\max}/E_{avg} varies inversely as the number of water droplets increases. The field intensification is much higher for 40° contact angle when compared to the contact angle of 170° as expected. As discussed in the previous chapter this behavior is due to the fact that acute and obtuse contact angles imply very low and very high degrees of hydrophobicities respectively.

3.4 Summary

In this Chapter electric field calculations were performed on the insulating surfaces for different patterns of wetting. The patterns varied with respect to a change in the number, relative position and contact angle of the water droplets. Simulations performed led to the following important outcomes.

- E-field intensity depends on the distance between the water droplets and the electrodes and also on the relative distance between two water droplets.
- Water droplets present in a row reduces the dry region between water droplets and results in high stress values.
- The location of the water droplet is more significant when compared with the number of water droplets.
- Hydrophobicity plays an important role in reducing the E-field intensity.

CHAPTER 4

ELECTRIC FIELD COMPUTATION OF WATER DROPLETS ON A PRACTICAL INSULATOR

4.1 Motivation

The simulations conducted in the previous chapters studied the electric field variations with respect to the contact angle, number and position of the water droplet on the model insulator. The present Chapter focuses on studying the behavior of the water droplets/films on a practical 138KV high voltage insulator. A dielectric with intrinsic hydrophobic property curbs the formation of water films. Instead discrete water droplets are formed that pose less danger to the performance of the insulator when compared with the water films. Thus, mainly two cases are investigated in the current work. The first case analyzes the hydrophobic case with discrete single and multiple water droplets on the shed and the sheath regions. Water droplets with contact angle of 90^0 are considered to perform the simulations. The second case refers to complete diminution of the hydrophobic property wherein water droplets coalesce and form a film on the surface of the insulator. For comparison purposes, a dry case with no water droplets is also analyzed.

4.2 Model Setup

The station posts available in the market come in different sizes or different number of sections with metal being the intermediate hardware to connect these sections [53]. The number of sections for high voltage insulators varies from one to four. A single

section has been considered here for simplicity. Due to the axi-symmetric nature of the insulator only a segment of the surface is modeled for simulation purposes.

As mentioned above a 138KV high voltage insulator was used to perform the simulations, which is shown in the Figure 4.1 below where 'a' is the shed region and 'b' is the sheath region.

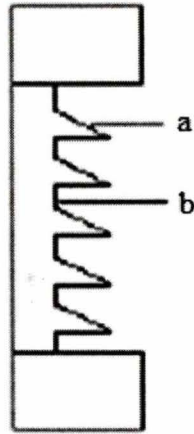


Figure 4.1 High Voltage Post Insulator (138 KV). ('a' represents the shed region and 'b' represents the sheath region)

The dimensions of the insulator are as follows. The vertical height of the insulator between the electrodes is 480 mm, the sheath and the shed diameter is 246 mm and 155 mm respectively. The shed spacing is 55 mm. The relative dielectric constant of the SIR is taken as 4.3 and its conductivity is taken as $1.0e^{-4}$. The water droplets considered have a diameter of 4mm with a contact angle of 90° . The relative dielectric constant of water is taken as 80 and its conductivity is $2.0e^{-4}$ mho/meter.

The definitude of the results in the 3D software Coulomb depends on the shape and the number of boundary elements used. Triangular shaped elements tend to perform better when compared to the quadrilateral elements. This has been proved by the author in [2]. The author also states that there is an increase in the accuracy with the increase in

the number of elements. Ten thousand triangular elements gave us acceptable results in our case.

4.3 Results and Analysis

The simulation results and analysis of the dry case, hydrophobic case and the complete loss of hydrophobicity or the hydrophilic case are presented in the sections below.

4.3.1 E-field in the Case of a Dry Insulator

The first case considered was the dry case with no water droplets present on the insulator surface. The Figure 4.2 shows the electric field distribution along the insulator length in the dry case.

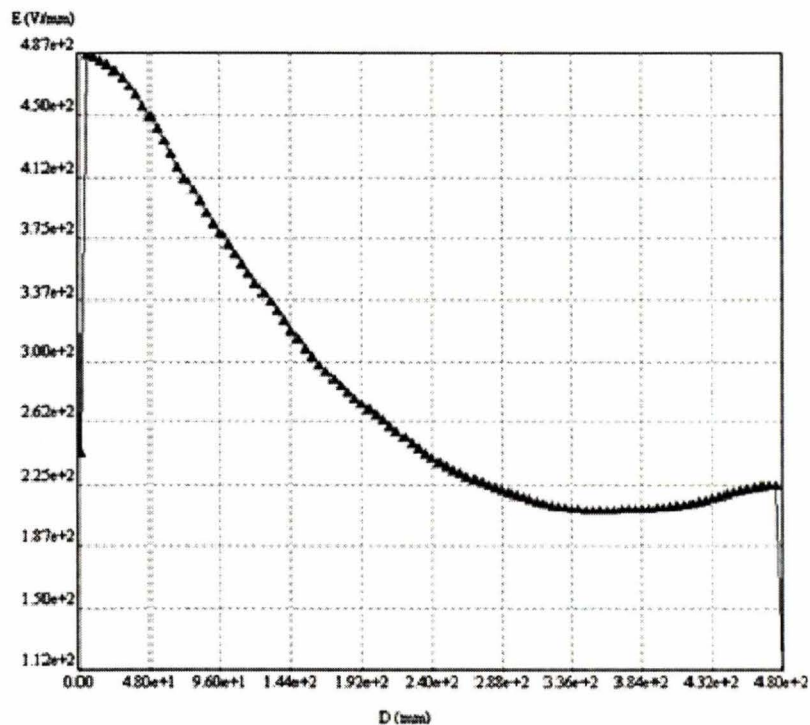


Fig 4.2 Electric Field Distribution along the Insulator Length in the Dry Case

When the produced electric field is beyond a certain critical value a conductive gas channel is formed due to which electrical breakdown occurs [54]. Thus a breakdown criterion is required to determine the whether the produced E-field value is calamitous for the insulator or not. The streamer breakdown criterion is generally accepted as the tool to calculate the inception or the breakdown voltage of gas gaps under various pressures and electric field distributions [55].

The electric field for initiating streamer is known to vary from 400-1150V/mm [53]. Hence the streamer threshold voltage in our simulations is taken to be 500V/mm. The Figure 4.2 shows that there is an exponential decrease in the E-field intensity and that the electrical stresses are the highest in the region adjacent to the high voltage electrode fitting. This behavior is attributed to the basic law of electric field.

The maximum electric field in the dry case is 487V/mm. Since the maximum stress is less than 500V/mm, it can be inferred that the probability of initiation of streamer mechanism is very low. This implies that electric field distribution is of little concern on a dry insulator.

4.3.2 E-field in Hydrophobic Case (Single and Multiple Water Droplets Case)

Discharges are initiated during wet conditions. Whether this results in flashover depends on the resistance of the unbridged portion of the insulator in series with the arc [56]. This is crucial since once the streamer breakdown is initiated the arc bridges the tip of the sheds in the shortest path possible and hence the leakage distance is completely ignored. It is the intent of this work to see how the presence of the water droplets causes the maximum stress to exceed the streamer threshold. Six cases were considered to study the effect of the water droplets on the surface of the insulator. They are (i) single water

droplet on the shed regions, (ii) single water droplet on the sheath regions, (iii) three water droplets on each of the shed regions, (iv) three water droplets on each of the sheath regions, (v) a single water droplet on both the shed and the sheath regions and (vi) three water droplets on each of the shed and the sheath regions respectively. Here three water droplets are placed in a column.

The Figure 4.3 depicts the model used to conduct field calculations of the first case i.e. a single water droplet is present on each of the shed regions. Five other models similar to this are constructed with a variation in the number of water droplets and simulations are performed.

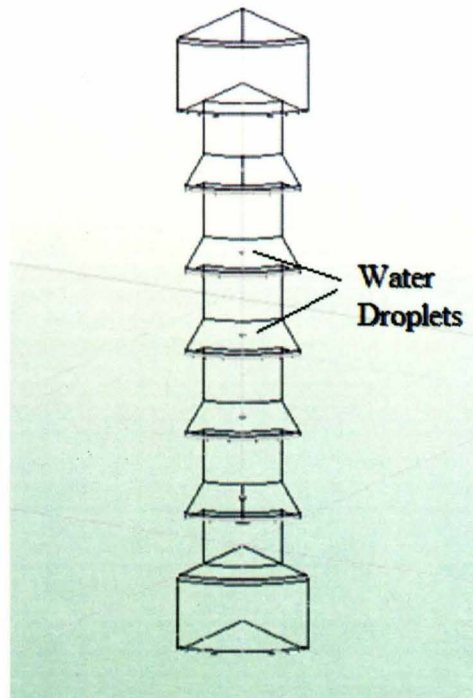


Fig 4.3 Single Water Droplets Placed on High Voltage Insulator (138 KV)

The Figure 4.4 shows the electric field distribution along insulator length when single water droplets are placed on each shed of the insulator. The enhancement of electric field value at the air – polymer interface or the triple points is represented by the

spikes in the Figure 4.4. In this case the maximum E-field value observed is 669V/mm. This value is higher when compared with the E_{\max} value of the dry case and it has exceeded the streamer threshold voltage by a significant amount. A streamer gets initiated when the E_{\max} exceeds the streamer breakdown voltage. The tips of the sheds in the air form the shortest path and thus the induced streamer jumps across the tips instead of following the leakage path [56]. This illustrates that during wet conditions discharges can readily occur.

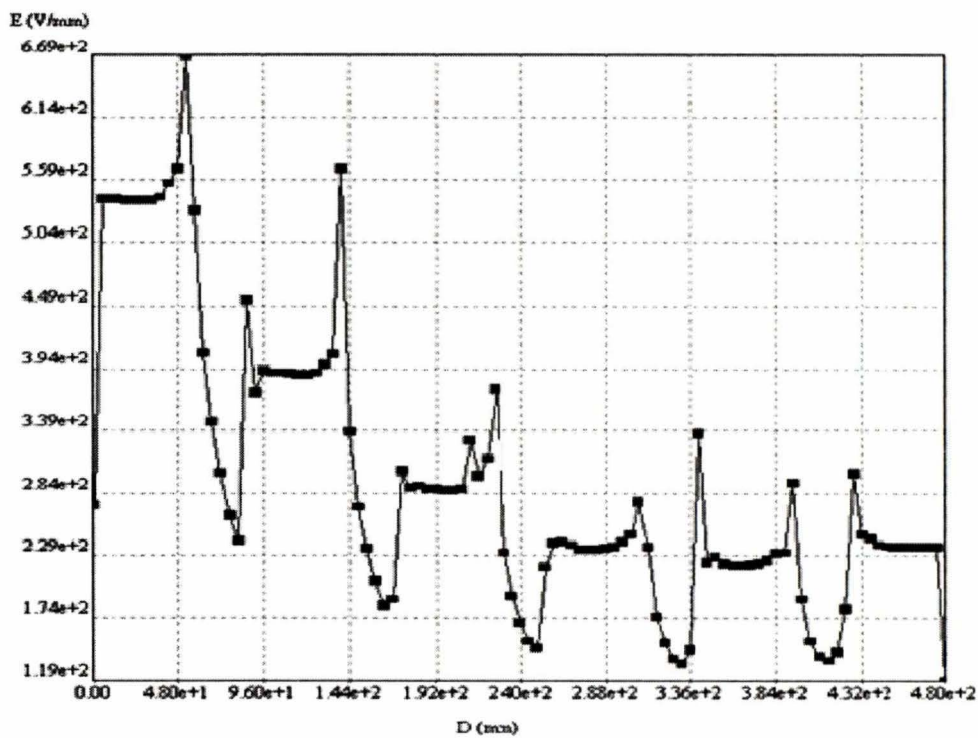


Figure 4.4 Electric Field Distribution Due to the Presence of Single Water Droplets on the Shed Region

The maximum electric field value is calculated for the other five cases and the E_{\max} values for all the six cases are represented in the form of a graph in Figure 4.5.

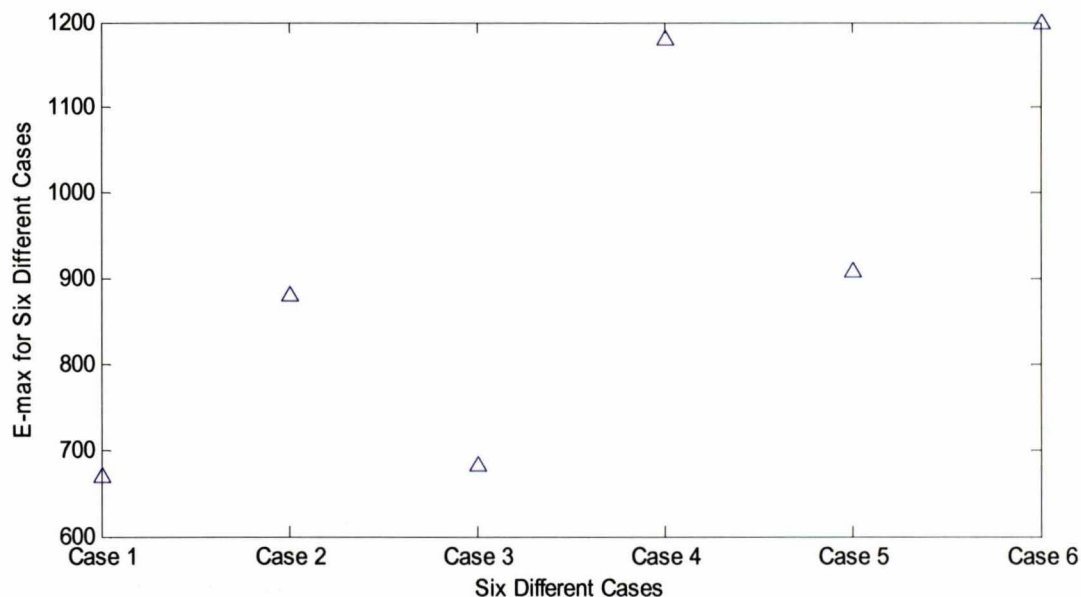


Fig 4.5 E_{\max} Values for Six Different Cases (the triangles in the figure represent the maximum electric field for six cases)

From Figure 4.5 the following observations are made. The triangles represent the maximum electric field for six cases.

- Case 1: one water bubble on the shed regions, E_{\max} - 669V/mm.
- Case 2: one water bubble on the sheath regions, E_{\max} - 881V/mm.
- Case 3: three water bubbles on the shed regions, E_{\max} - 682V/mm.
- Case 4: three water bubbles on the sheath regions, E_{\max} - 1180V/mm.
- Case 5: one water bubble on each of the shed and sheath regions, E_{\max} - 909V/mm.
- Case 6: three water bubbles on each of the shed and sheath regions, E_{\max} - 1200V/mm

The E_{\max} values obtained in Figure 4.5 indicate that the electric field intensification is at the maximum for case six where three water droplets exist on each of

the shed and the sheath regions of the insulator. The case with single water droplets on each of the shed regions exhibited minimum amounts of electric field intensification. The E_{\max} values exceeded the streamer breakdown voltage in all of the six cases. However the margin of difference with respect to streamer threshold voltage is high in the second, fourth and the sixth cases, implying that these conditions are more prone to the occurrence of flashover.

Analysis

The sheath part attributing to its narrow dimension encounters higher amount of stress in comparison with the broader shed region. Along the sheath the electric field exerted on water droplets is tangential to the surface of the insulator which will lead to elongation of the water droplet into an ellipsoidal shape. This phenomenon increases the electric field intensity by a significant amount and high stress concentration is observed at the triple point (insulator, air and water droplet) on the sheath region [57]. The electric stresses produced on the shed are perpendicular in direction and therefore E-field intensification occurs at the top of the water droplet away from the insulator surface. Thus, electric field intensification is relatively less on the shed regions [38]. This implies that emission of electrical discharges and subsequent occurrence of flashover gets initiated at the sheath regions and the discharges on the shed region may not have a critical impact on the performance of the insulator. This is observed in the results obtained i.e. E_{\max} in Case 2 is high when compared with E_{\max} in Case 1.

In practice a number of water droplets are present on the surface of the insulator and each additional drop would contribute in increasing the stress along the surface of the insulator. Moreover it would have an influence on each other as well. This makes the

effect of water droplets very complex [50]. To understand the behavior of multiple water droplets Case 3 is considered. Three water droplets are placed one below the other in a column. An increase in the value of E_{\max} is observed in Case 3 when compared with Case 1 where only a single water droplet is placed. This occurs due to the following reason. Presence of water droplets one below the other significantly reduces the dry region and causes the voltage to be distributed amongst the available dry regions between them. The water droplets then attain the potential of the equipotentials passing through them and act as conducting particles aligned along the field direction resulting in enhanced electric stresses locally [56]. A comparison between the E_{\max} values of Case 2 and Case 3 indicates that a single water droplet on the sheath region is of more concern when compared with three water droplets on the shed part of the insulator. Case 4 simulated three water droplets on the sheath region and the obtained E_{\max} value is nearly twice to that of Case 2. This result demonstrates that an increase in the number of water droplets on the sheath region proves to have more effect on the E-field intensification.

Previously done work mentioned in Chapters 1 and 2 studied the behavior of the water droplets on the shed and the sheath regions separately. In practical scenario water droplets may be present on both the shed and the sheath regions. Case 5, with a single water droplet on both the shed and the sheath region is considered to understand the importance of this situation. Case 5 exhibited a small amount of increase in the value of E_{\max} when compared with Case 2 where single water droplets are present only on the sheath region. Case 6 included three water droplets on both the shed and the sheath regions. Figure 4.5 shows that there has been no significant increase in the value of E_{\max}

indicating that presence of single water droplets are as hazardous as the presence of multiple water droplets.

4.3.3 E-field in Hydrophilic Case (with Water Films on the Shed Region)

Hydrophobicity is the water repellent characteristic of the insulator and a loss of the property will lead to the formation of water films instead of discrete water droplets. This results in a completely wet insulating surface and enhances the probability of the occurrence of flashover [57]. To analyze the gravity of this situation very thin water films with a height of 1mm are considered on the shed region. The Figure 4.6 shows the model designed in Coulomb to calculate the E-field values.

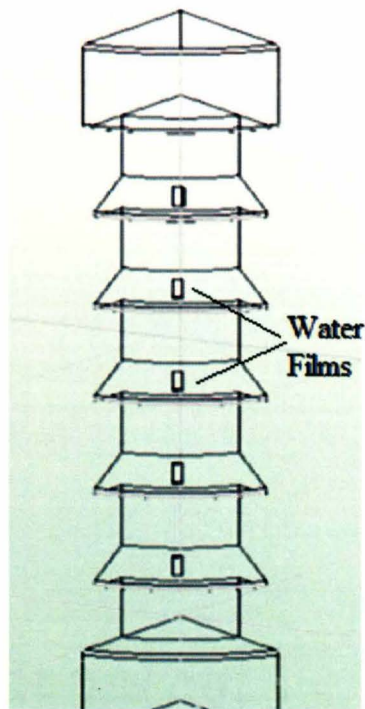


Fig 4.6 Water Films Placed on the Shed Regions

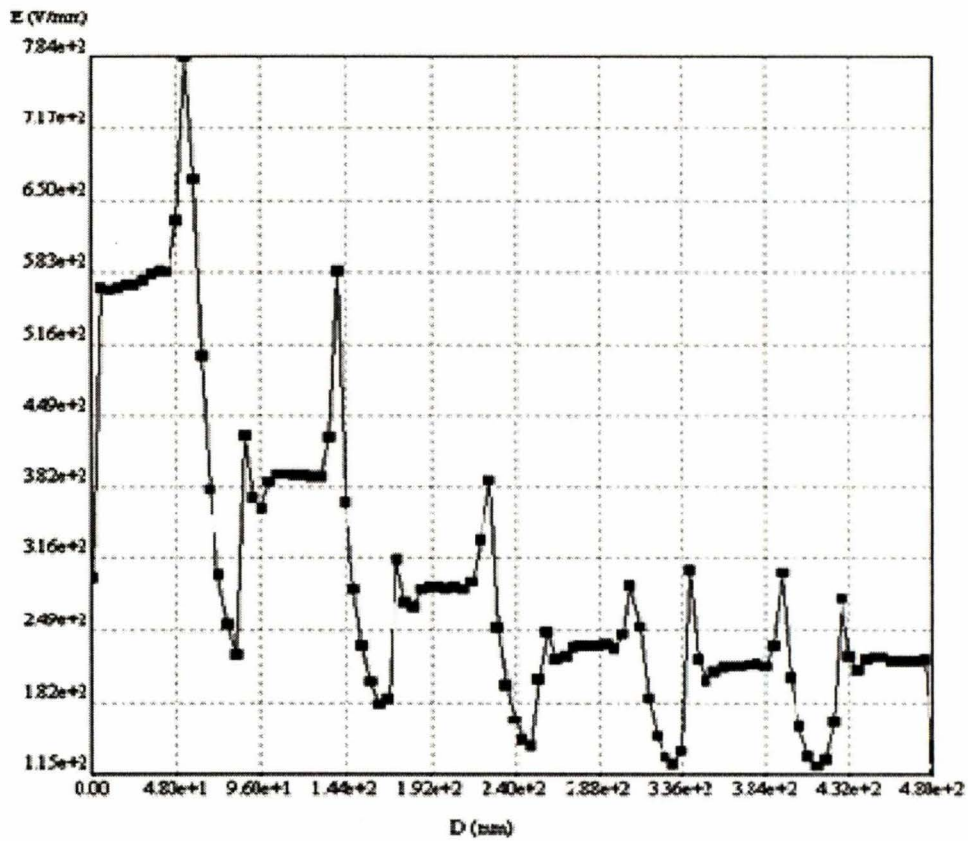


Fig 4.7 Electric Field Distribution Due to the Presence of Water Films on the Shed Regions

The Figure 4.7 shows the electric field distribution obtained due to the presence of water films on the shed region of the insulator. E_{\max} value of 784V/mm is observed. The value exceeds both the streamer threshold value of 500V/mm and the Case 1 where single water droplets are present on the shed region. This behavior indicates that insulating surfaces with moderate level of hydrophobicity (90° contact angle) are less dangerous when compared with hydrophilic surfaces. Thus hydrophobicity can be considered to be a pivotal factor in increasing the lifetime of the insulator.

4.4 Summary

In this Chapter, two cases namely hydrophobic and hydrophilic cases were analyzed on a 138 KV high voltage practical insulator. The hydrophobic case considered six different scenarios to obtain a better understanding of the effect of single and multiple water droplets on the shed and the sheath regions of the insulator. The effect of loss of hydrophobicity is observed with the aid of thin water films on the shed regions. The simulation results indicate the following.

- A water droplet on the sheath region enhances the electric field intensity to a large extent.
- The dry region is reduced due to the presence of multiple water droplets and subsequently results in an increase of electric field stresses between water droplets.
- The E-field intensification at the triple points of the water films is significantly high when compared with the electric stresses produced by the triple points of the water droplets. This concludes that the property of hydrophobicity aids in reducing the number of areas where E-field values exceed the streamer breakdown value.

CHAPTER 5

CONCLUSIONS AND FUTURE WORK

5.1 Conclusions of the Thesis

Water droplets/films on the surface of the insulator create high electrical stress areas and subsequently may lead to the electrical breakdown of an insulator. Electric field profiles around water droplets are crucial for designing and choosing a reliable insulating material. The amount of electric field intensification caused by water droplets/films depends on various factors. The current work aimed at investigating few of the many factors namely the effect of variation of hydrophobicity (contact angle), insulating material, number and relative positioning of the water droplets. Three different situations were considered with single/multiple water droplets/films and all the simulations were performed with the help of Coulomb, a 3D software tool. The Boundary Element Method (BEM) was the numerical method employed to obtain electric field calculations.

The results give rise to the following conclusions. The electric field intensity is relatively more at the sheath region of the insulator when compared to the shed region. The maximum electric field value varies with a variation in the contact angle. The variation of the insulating material indicated that silicone rubber provides better electrical performance in comparison with porcelain. Multiple water droplets also depend on the angle of contact in a similar manner. Furthermore additional stresses are built around the water droplets with respect to a change in the distance between the electrodes and water droplets and distance between each other. Water films are formed as a result of complete diminution of hydrophobicity and its effect on E-field intensification is more hazardous when compared with the discrete water droplets.

5.2 Future Work

Polymeric insulators have relatively more advantages when compared with the conventional ceramic insulators. The recent growth in demand and less on field experience urges the need for more research in non-ceramic insulators. The current work dealt with studying the effect of water droplets/films on a model insulator and a practical insulator comprising one section. However, in practice station post insulators contain several sections ranging from one to four depending on the voltage and metal hardware is used to connect the different sections. The additional length, voltage and metal hardware will affect the E-field distribution. A logical extension of the current work would be to study the effect of water droplets/films with a variation in the number of sections.

In addition, the profile of the insulator is another factor that greatly influences the electrical performance of the insulator. Researchers have been concentrating mainly on improving the chemical composition of the non-ceramic insulators and there has not been much work done on the non-ceramic insulator profiles. Moreover considerable amount of work has not been done to evaluate the effect of water droplets on different non-ceramic insulator profiles. It would be beneficial to learn the effect of water droplets/films on different insulator profiles. The profile of the insulator can be varied with respect to the change in leakage distance, shed profile, shed spacing etc. A hydrophobic non-ceramic insulator combined with an insulator profile which produces minimum amounts of stress would result in an optimum insulating device.

REFERENCES

- [1] J. S. T. Looms, *Insulators for High Voltages*, Peter Peregrinus Ltd., 1988.
- [2] M. N. Hussain, A. Arainy, M. I. Qureshi, *Electrical Insulation in Power Systems*, Marcel Dekker Inc., 1998.
- [3] R. S. Gorur, E. A. Cherney, J. T. Burnham, *Outdoor Insulators*, Ravi S. Gorur Inc., 1999.
- [4] F. Masoud, *Insulators for Icing and Polluted Environments*, IEEE Computer Society Press, 2009.
- [5] W. K. Chen, *The Electrical Engineering Handbook*, Academic Press, 2004.
- [6] F. T. Andrews, "The Heritage of Telegraphy", *IEEE Communication Magazine*, vol. 27, no. 3, pp. 12-18, August 1989.
- [7] W. L. Vosloo, J. P. Holtzhausen, A. H. A. Roediger., "Leakage Current Performance of Naturally Aged Non-ceramic Insulators under a Severe Marine Environment", *IEEE 4th AFRICON*, vol. 1, pp. 489-495, September 1996.
- [8] C. L. Wadhwa, *Electrical Power Systems*, New Age International Publishers, 2009.
- [9] S. Ray, *Electrical Power Systems: Concepts, Theory and Practice*, Prentice-Hall of India Pvt. Ltd., 2009.
- [10] N. Bashir, H. Ahmad, "Ageing of Transmission Line Insulators: The Past, Present and Future", *IEEE International Conference on Power and Energy*, pp. 30-34, 1-3 December 2008.

- [11] M. J. Owen, "Silicone Polymers for High Voltage Insulators", *Rubber World: The Technical Service Magazine for the Rubber Industry*, vol. 217, no. 3, pp. 287-292, December 1997.
- [12] H. M. Schneidner, J. F. Hall, G. Karady, J. Renowden, "Non-ceramic Insulators for Transmission Lines", *IEEE Transactions on Power Delivery*, vol. 4, no. 4, pp. 2214-2221, October 1989.
- [13] J. F. Hall, "History and Bibliography of polymeric Insulators for Outdoor Applications", *IEEE Transactions on Power Delivery*, vol. 8, no. 1, pp. 376-381, January 1993.
- [14] J. Mackevich, M. Shah, "Polymer Outdoor Insulating Materials. Part I: Comparison of Porcelain and Polymer Electrical Insulation", *IEEE Electrical Insulation Magazine*, vol. 13, no. 3, pp. 5-12, May 1997.
- [15] K. O. Papiliou "Composite Insulators are Gaining Ground—25 years of Swiss Experience," *IEEE Transmission and Distribution Conference*, vol. 2, pp. 827–833, 5-9 April 1999.
- [16] M. Amin, A. Mohammad, S. Amin, "Hydrophobicity of Silicone Rubber used for Outdoor Insulation (An Overview)", *IEEE Transactions on Dielectrics and Electrical Insulation*, vol. 1, no. 6, pp. 10-26, June 2007.
- [17] R. A. Bernstorf, D. Ryan, "Silicone Compounds for High Voltage Insulators: HPS Testing of Silicone Compounds", *Hubbell Power Systems Inc.*, 2007. [Online]. Available: <http://www.hubbellpowersystems.com>. [Accessed: August 17, 2009].

- [18] T. Braunsberger, A. Dziubek, M. Kurrat, "Water Drop Corona on Hydrophobic Epoxy", *IEEE International Conference on Solid Dielectrics*, vol. 1, pp. 439-444, 5-9 July 2004.
- [19] T. Zhao, J. Sakich, "Salt Fog Aging Tests on Non-Ceramic Insulators and Fog Chamber Data Acquisition System", *IEEE Conference on Electrical Insulation and Dielectric Phenomena*, vol. 1, pp. 377-380, 20-23 October 1996.
- [20] R. A. Bernstorf, R. K. Niedermier, D. S. Winkler, "Polymer Compounds used in High Voltage Insulators", *Hubbell Power Systems Inc.*, 2004. [Online]. Available: <http://www.hubbellpowersystems.com/literature/insulators/EU1407.pdf>. [Accessed: August 20, 2009].
- [21] P. J. Smith, M. J. Owen, P. H. Holm, G. A. Toskey, "Surface Studies of Corona-treated Silicone Rubber High-voltage Insulation," *IEEE Conference on Electrical Insulation and Dielectric Phenomena*, pp. 829-836, 18-22 October 1992.
- [22] J. Kindersberger, M. Kuhl., "Effect of Hydrophobicity on Insulator Performance," *Conference on Electrical Insulation and Dielectric Phenomena*, vol. 1, pp. 226-229, June 2000.
- [23] L. Grigsby, *Electric Power Generation, Transmission, and Distribution*, CRC Press, 2007.
- [24] F. Kapper, *Overhead transmission lines and distributing circuits: Their design and construction*, D. Van Nostrand Company, 1915.

- [25] S. Han, H. Cho, I. Choi, D. Lee, "Failure Characteristics of Suspension-Type Porcelain Insulators on a 154kV Transmission Line," *Conference Record of the 2006 IEEE International Symposium on Electrical Insulation*, pp. 118-121, 11-14 June 2006.
- [26] M. S. Naidu, *High Voltage Engineering*, McGraw-Hill Professional Publishing, 1995.
- [27] L. Kennedy, A. Fridman, *Plasma Physics and Engineering*, CRC Press, 2004.
- [28] J. A. Rees, *Electrical Breakdown in Gases*, Wiley Publications, 1973.
- [29] R. S. Gorur, R. Olsen, "Prediction of Flashover Voltage of Insulators Using Low Voltage Surface Resistance Measurement," *Power Systems Engineering Research Center*, 2006. [Online]. Available: <http://www.pserc.wisc.edu>. [Accessed: October 11, 2009].
- [30] H. Raether, *Electron Avalanches and Breakdown in Gases*, Butterworths, 1964.
- [31] M. T. Gencog Lu, M. Cebeci, "Investigation of Pollution Flashover on High Voltage Insulators Using Artificial Network," *Journal of Expert Systems with Applications*, vol. 36, no. 4, pp. 7338-7345, August 2009.
- [32] G. Karady, "Flashover Mechanism on Non-ceramic Insulators," *IEEE Transactions on Dielectrics and Electrical Insulation*, vol. 6, no. 5, pp. 718-723, October 1999.
- [33] J. Liebermann, "New Effective Ways towards Solving the Problem of Contamination of Porcelain Insulators," *Journal of Refractories and Industrial Ceramics*, vol. 43, nos. 1-2, pp. 55-64, June 2002.

- [34] K. C. Hotle, "Application of Insulators in a Contaminated Environment," *IEEE Transactions on Power Apparatus and Systems*, vol. 98, no. 5, pp. 1676-1685, October 1979.
- [35] A. H. El-Hag, S. H. Jayaram, E. A. Cherney, "Calculation of Leakage current density of silicone rubber insulators under accelerated aging conditions," *Journal of Electrostatics*, vol. 67, no. 4, pp. 48-53, October 2009.
- [36] A. H. El-Hag, S. H. Jayaram, E. A. Cherney, "Effect of Insulator Profile on Aging Performance of Silicone Rubber Insulators in Salt," *IEEE Transactions on Dielectrics and Electrical Insulation*, vol. 14, no. 2, pp. 352-359, April 2007.
- [37] R. S. Gorur, E. A. Cherney, R. Hackam, "Polymer Insulator Profiles Evaluated in a Fog Chamber," *IEEE Transactions on Power Delivery*, vol. 5, no. 2, pp. 1078-1085, April 1990.
- [38] P. Basappa, V. K. Lakdawala, B. Sarang, A. Mishra, "Simulation of Electric Field Distribution around Water Droplets on Outdoor Insulator Surfaces," *Conference Record of IEEE International Symposium on Electrical Insulation*, pp. 50-54, 9-12 June 2008.
- [39] A. M. Imao, A. Beroual, "Deformation of Water Droplets on Solid Surface in Electric Field," *Journal of Colloid and Interface Science*, vol. 228, no. 12, pp. 869-879, August 2006.
- [40] K. Parraud, "Comparative Electric Field Calculations and Measurements on High Voltage Insulators", *European Transactions on Electrical Power*, vol. 19, no. 3, pp. 69-77, April 1992.

- [41] N. H. Malik, "A Review of the Charge Simulation Method and its Applications", *IEEE Transactions on Electrical Insulation*, vol. 24, no. 1, pp. 3-20, February 1989.
- [42] G. D. Smith, *Numerical Solution of Partial Differential Equations: Finite Difference Methods*, Oxford University Press, 1986.
- [43] D. W. Pepper, J. C. Heinrich, *The Finite Element Methods: Basic Concepts and Applications*, Taylor and Francis Group, 1992.
- [44] L. C. Wrobel, *The Boundary Element Method: Applications in Thermo –Fluids and Acoustics*, John Wiley and Sons, 2002.
- [45] M. A. Jaswon, T. T. Symm, *Integral Equation Methods in Potential Theory and Electrostatics*, Academic Press, 1977.
- [46] Q. Weiguo, S. A. Sebo, "Electric Field and Potential Distributions along Non-Ceramic Insulators with Water Droplets", *Electrical Insulation Conference and Electrical Manufacturing & Coil Winding Conference*, pp. 441-444, June 2001.
- [47] I. Gutman, "STRI Guidelines for Diagnostics of Composite Insulators: For Visual Inspections; For Hydrophobicity; For IR Helicopter Inspections", *International Conference of Suspension and Post Composite Insulators: Manufacturing, Technical Requirements, Test methods, Service Experience, Diagnostics*, pp. 88-91, October 2004.
- [48] A. M. Imano, A. Beroual, "Electric Field Simulation of Water Droplets on Solid Surface in Electric Field", *Journal of Colloid and Interface Science*, vol. 4, no. 2, pp. 169-175, June 2006.

- [49] Z. Guan, L. Wang, B. Yang, X. Liang, "Electric Field Analysis of Water Drop Corona", *IEEE Transactions on Power Delivery*, vol. 20, no. 2, pp. 964-969, April 2005.
- [50] Y. Zhu, K. Haji, M. Otsubo, C. Honda, N. Hayashi, "Electrohydrodynamic Behaviour of Water Droplet on a Electrically Stressed Hydrophobic Surface", *Journal of Applied Physics*, vol. 39, no. 3, pp. 1970-1975, June 2006.
- [51] A. J. Philips, D. J. Childs, H. M. Schneider, "Aging of Non-ceramic Insulators due to Corona from Water Droplets", *IEEE Transactions on Power Delivery*, vol. 14, no. 3, pp. 1081-1089, July 1999.
- [52] B. Sarang, V. Lakdawala, P. Basappa, "Electric Field Calculations of Wet Insulating Surfaces", *IEEE Conference on Electrical Insulation Dielectric Phenomena*, pp. 228-231, 26-19 October 2008.
- [53] K. Sheno, R. S. Gorur, "Evaluating Station Post Insulator Performance from Electric Field Calculations", *IEEE Transactions on Dielectrics and Electrical Insulation*, vol. 15, no. 6, pp. 1731-1738, December 2008.
- [54] G. A. Greene, Y. I. Cho, A. Cohen, J. P. Hartnett, *Advances In Heat Transfer*, Academic Press, 2006.
- [55] K. Petcharaks, "A contribution to the Streamer Breakdown Criterion", *Eleventh International Symposium on High Voltage Engineering*, vol. 3, pp. 19-22, August 1999.
- [56] B. Sarang, V. Lakdawala, P. Basappa, "Electric Field Calculations on a High Voltage Insulator under Wet Conditions", *IEEE Electrical Insulation Conference*, pp. 86-90, 1-4 June 2009.

- [57] Y. Higashiyama, S. Yanase, T. Sugimoto, "DC Corona Discharge from Water Droplets on a Hydrophobic Surface", *Journal of Electrostatics*, vol. 55, no. 3, pp. 351-360, July 2002.

Bhargavi Sarang

Department of Electrical and Computer Engineering
Old Dominion University
757-652-5214
bsara001@odu.edu

Education

Master of Science in Electrical Engineering, May 2010 (GPA-3.75)

Old Dominion University, Norfolk, VA

B.Eng. (HONS) in Electronics and Communication Engineering, May 2005 (GPA-3.5)

University of Wolverhampton, United Kingdom.

Related Experience

Old Dominion University, Norfolk, VA.

- Tutor for Math, Physics and Chemistry (Fall 2008 – Spring 2010).
- Graduate Assistant (Fall 2008 – Spring 2009)

Research Publications

Conference Papers:

P. Basappa, V. K. Lakdawala, B. Sarang, A. Mishra, “ Simulation of Electric Field Distribution around Water Droplets on Outdoor Insulator Surfaces,” *Conference Record of IEEE International Symposium on Electrical Insulation*, pp. 50-54, 9-12 June 2008.

B. Sarang, V. Lakdawala, P. Basappa, “Electric Field Calculations of Wet Insulating Surfaces”, *IEEE Conference on Electrical Insulation Dielectric Phenomena*, pp. 228-231, 26-19 October 2008.

B. Sarang, V. Lakdawala, P. Basappa, “Electric Field Calculations on a High Voltage Insulator under Wet Conditions”, *IEEE Electrical Insulation Conference*, pp. 86-90, 1-4 June 2009.

Professional Achievements

- Successfully presented four IEEE conference papers.
- Organized many events at Shruthi (Chaitanya Bharathi Institute of Technology, India).
- Volunteered for Bhoomi (a social services organization in India).
- School captain for the year 1999-2000 in High School

Personal Strengths

- Team player with good communication and managerial skills.
- Ability to adapt new environments and learn quickly.
- Hard working and amicable.